nature medicine

Article

https://doi.org/10.1038/s41591-025-03575-0

Nivolumab plus chemotherapy or ipilimumab in gastroesophageal cancer: exploratory biomarker analyses of a randomized phase 3 trial

Received: 8 May 2024

Accepted: 7 February 2025

Published online: 7 March 2025

Check for updates

A list of authors and their affiliations appears at the end of the paper

First-line nivolumab-plus-chemotherapy demonstrated superior overall survival (OS) and progression-free survival versus chemotherapy for advanced gastroesophageal adenocarcinoma with programmed death ligand 1 combined positive score ≥ 5, meeting both primary end points of the randomized phase 3 CheckMate 649 trial. Nivolumab-plus-ipilimumab provided durable responses and higher survival rates versus chemotherapy; however, the prespecified OS significance boundary was not met.
To identify biomarkers predictive of differential efficacy outcomes, post hoc exploratory analyses were performed using whole-exome sequencing and RNA sequencing. Nivolumab-based therapies demonstrated improved efficacy versus chemotherapy in hypermutated and, to a lesser degree, Epstein–Barr virus-positive tumors compared with chromosomally unstable and genomically stable tumors. Within the KRAS-altered subgroup, only patients treated with nivolumab-plus-chemotherapy demonstrated improved OS benefit versus chemotherapy. Low stroma gene expression signature scores were associated with OS benefit with nivolumab-based regimens; high regulatory T cell signatures were associated with OS benefit only with nivolumab-plus-ipilimumab. Our analyses suggest that distinct and overlapping pathways contribute to the efficacy of nivolumab-based regimens in gastroesophageal adenocarcinoma.

Integration of immune checkpoint blockade into the therapeutic armamentarium of advanced gastroesophageal adenocarcinoma has improved outcomes in a disease where standard first-line chemotherapy has median OS of less than 1 year[1–4]. Nivolumab, a programmed death 1 (PD-1) inhibitor, plus chemotherapy, demonstrated superior OS compared with chemotherapy alone in previously untreated, nonhuman epidermal growth factor receptor 2 (HER2)-positive advanced gastric, gastroesophageal junction and esophageal adenocarcinoma in the CheckMate 649 study[5]. Based on these data, nivolumab-plus-chemotherapy is approved for the first-line treatment of this disease in many countries[6]. In contrast, treatment with nivolumab plus the cytotoxic T lymphocyte antigen-4 (CTLA-4) inhibitor ipilimumab failed to meet the prespecified hierarchically tested secondary end point of OS versus chemotherapy in patients with programmed death ligand 1 (PD-L1) combined positive score (CPS) ≥ 5, although responses were more durable and the OS rate was higher at 24 months[7].

Nivolumab and ipilimumab elicit antitumor responses by distinct but complementary mechanisms of action[8,9]. PD-1 inhibition restores the antitumor function of T cells[10], whereas CTLA-4 inhibition induces de novo antitumor T cell responses as well as modulation of regulatory T cells[11–14]. Anti-PD-1 and anti-CTLA-4 combination therapies

e-mail: janjigiy@mskcc.org; ming.lei1@bms.com

https://doi.org/10.1038/s41591-025-03575-0

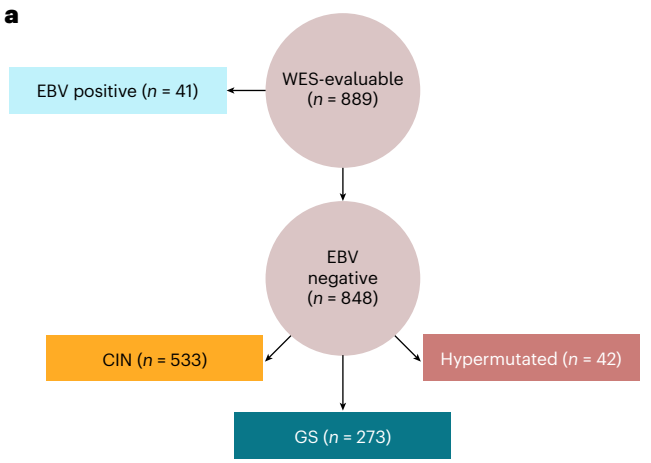

WES cluster, *n* (%)	CIN	GS	Hypermutated	EBV	Total
MSS	528 (63)	271 (32)	5 (1)	40 (5)	844 (100)
MSI-H	3 (7)	0 (0)	37 (90)	1 (2)	41 (100)
NA	2 (50)	2 (50)	0 (0)	0 (0)	4 (100)
Total	533 (60)	273 (31)	42 (5)	41 (5)	889 (100)

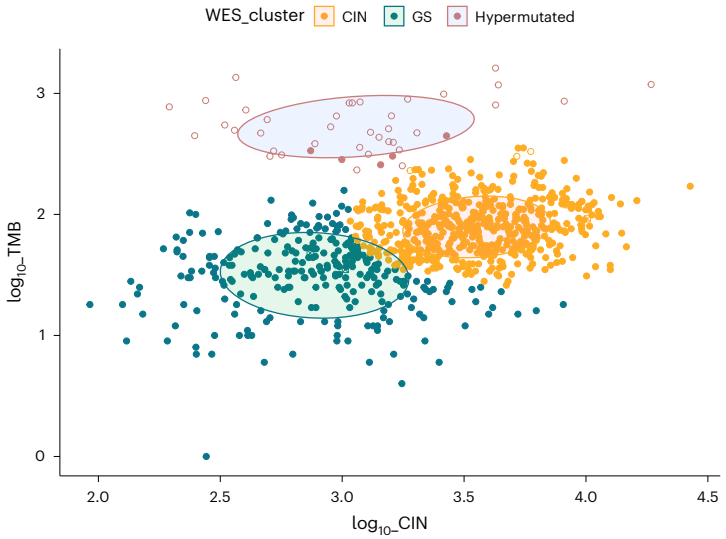

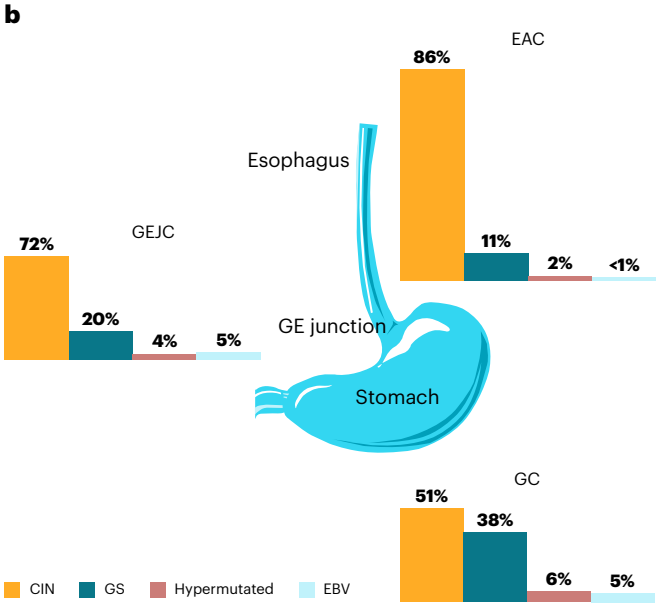

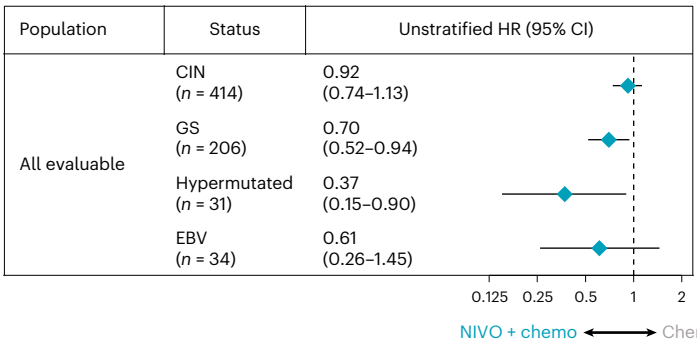

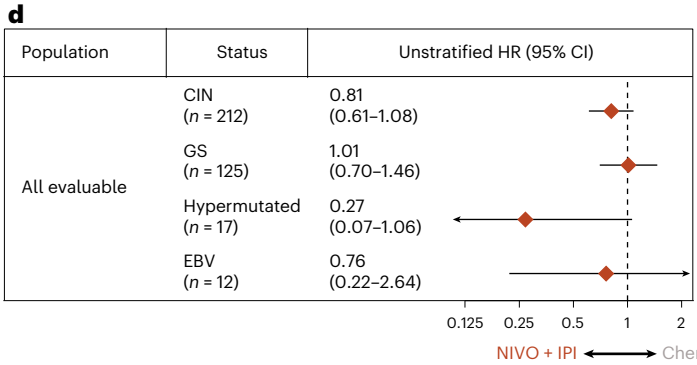

Fig. 1 | Genomic characterization of baseline tumors from CheckMate 649. **a**, Flowchart depicting method of genomic classification of tumors (left). Scatter-plot of TMB versus genomic instability in EBV-negative tumors (right). **b**, Tumor subtyping by anatomical location. **c**,**d**, Forest plot of OS by genomic subsets in patients treated with nivolumab-plus-chemotherapy (**c**) or nivolumab-plus-ipilimumab (**d**) versus chemotherapy. Data are presented as unstratified HRs and 95% CI. HR was not calculated if the number of patients in each arm was <5. Open circles represent MSI-H, filled circles represent MSS, and squares represent not available (NA). IPI, ipilimumab; MSI-H, MSI-high; NIVO, nivolumab.

enhance expansion of tumor-specific T cells, including $CD8^+$ T cells and T helper cells, compared with monotherapies[8,15]. The observed efficacy of nivolumab-plus-chemotherapy in CheckMate 649 may be attributed to the potentiation of chemotherapy-induced cytotoxicity and immunogenic cell death with the antitumor effects of nivolumab[16]. Therefore, responses to nivolumab-plus-chemotherapy and to nivolumab-plus-ipilimumab are likely driven by distinct molecular or immunophenotypes of the tumor. Identification of pretreatment biomarkers associated with outcomes with nivolumab-based regimens in gastroesophageal adenocarcinoma may help identify patient subgroups that are likely to derive the most clinical benefit.

Among the four molecularly distinct subsets of gastroesophageal cancer[17], microsatellite instability (MSI)-high tumors have the most favorable outcomes with immune checkpoint blockade, whereas

studies describing tumors with chromosomal instability (CIN) or that are genomically stable (GS) or Epstein–Barr virus (EBV)-positive are limited[18–21]. Select gene expression signatures (GES) related to inflammation, stroma or angiogenesis were associated with immune checkpoint blockade outcomes across tumor types[22–31]; however, there has not been a comprehensive DNA or RNA analysis exploring the relationship of various pretreatment tumor characteristics with therapeutic outcomes in metastatic gastroesophageal adenocarcinoma. We describe in-depth biomarker analyses from baseline tumors from the CheckMate 649 study to examine the association of biomarkers with survival outcomes in patients treated with nivolumab-plus-chemotherapy or nivolumab-plus-ipilimumab versus chemotherapy.

Results

Patient population

Of 1,581 patients randomized to receive nivolumab-plus-chemotherapy versus chemotherapy, 685 (43%) were evaluable by whole-exome sequencing (WES) and 809 (51%) were evaluable by RNA sequencing (RNA-seq) (Supplementary Table 1). Of 813 patients randomized to receive nivolumab-plus-ipilimumab versus chemotherapy, 366 (45%) were evaluable by WES and 402 (49%) were evaluable by RNA-seq (Supplementary Table 2). At data cutoff (31 May 2022), minimum follow-up (time from concurrent randomization of the last patient to data cutoff) for the nivolumab-plus-chemotherapy versus chemotherapy group was 36.2 months. Minimum follow-up for the nivolumab-plus-ipilimumab versus chemotherapy group was 47.9 months.

Baseline characteristics were generally balanced between the treatment groups and were consistent for all-randomized, WES-evaluable and RNA-seq-evaluable patients (Supplementary Tables 1 and 2). Median OS and hazard ratios (HRs) were generally comparable between all-randomized, WES-evaluable and RNA-seq-evaluable patients in both the nivolumab-plus-chemotherapy and nivolumab-plus-ipilimumab versus chemotherapy groups, suggesting that the biomarker-evaluable populations were representative of the entire randomized population (Supplementary Tables 1 and 2).

OS by genomic subtypes

Among the WES-evaluable population (n = 889), 41 patients (5%) were EBV positive. Of tumors that did not have sequences mapping to the EBV genome, a Gaussian mixture model of tumor mutational burden (TMB) and CIN scores identified three clusters: 533 (60%) had a high chromosomal instability score and were classified as CIN, 273 (31%) had low chromosomal instability score and were classified as GS and 42 (5%) had high TMB and were classified as hypermutated (Fig. 1a). These subtypes were in alignment with those described by The Cancer Genome Atlas (TCGA)[17]. Further characterization revealed that 37 of 42 (88%) hypermutated tumors were MSI-high (Fig. 1a). Analysis of the genomic subtypes by tumor location revealed that the CIN subtype was predominant in esophageal (86%) and gastroesophageal junction adenocarcinomas (72%) (Fig. 1b). Association with histology was consistent with TCGA[17], and the diffuse histological subtype was predominant in the GS group (Extended Data Fig. 1a). Although the prevalence of PD-L1 CPS ≥ 5 was high in the EBV subtype, no pronounced associations were seen with PD-L1 CPS and genomic subtypes (Extended Data Fig. 1b).

The hypermutated subtype benefited most from both nivolumab-based regiments versus chemotherapy (nivolumab-plus-chemotherapy, HR 0.37, 95% CI 0.15–0.90; Fig. 1c; nivolumab-plus-ipilimumab, HR 0.27, 95% CI 0.07–1.06; Fig. 1d).

Patients with CIN subtype derived less benefit from the addition of nivolumab to chemotherapy (HR 0.92, 95% CI 0.74–1.13) compared with those with GS (HR 0.70, 95% CI 0.52–0.94) or EBV (HR 0.61, 95% CI 0.26–1.45) subtypes (Fig. 1c); similar OS trends across these subtypes were also observed in the PD-L1 CPS ≥ 5 population (Extended Data Fig. 1c); however, a different trend was observed with nivolumab-plus-ipilimumab versus chemotherapy, which resulted in an HR of 0.81 (95% CI 0.61–1.08) in the CIN subtype and 0.76 (95% CI 0.22–2.64) in the EBV subtype compared with 1.01 (95% CI 0.70–1.46) in the GS subtype.

OS by TMB and MSI status

Among WES-evaluable patients treated with nivolumab-plus-chemotherapy, 57 patients (8%) were TMB-high (TMB-high denotes ≥199 mutations/exome; Fig. 2a). An analysis of the association between TMB and microsatellite instability in patients where both biomarkers were evaluable revealed that all patients with MSI-high tumors also had TMB-high status.

The magnitude of OS benefit seemed higher with nivolumab-plus-chemotherapy versus chemotherapy in patients with TMB-high tumors (HR 0.48, 95% CI 0.25–0.91) compared with those with TMB-low tumors (HR 0.85, 95% CI 0.72–1.00). A similar trend was observed when MSI-high patients were excluded from the analysis, suggesting that the association was not solely driven by MSI-high patients (Fig. 2a). The enrichment of OS benefit in TMB-high tumors with nivolumab-plus-chemotherapy versus chemotherapy was consistently observed in patients with PD-L1 CPS ≥ 5 tumors (HR 0.43, 95% CI 0.21–0.89; Extended Data Fig. 2a). The number of patients with TMB-high and PD-L1 CPS < 5 was less than 5 per treatment group; therefore, OS benefit could not be evaluated. In patients with MSI-high tumors, the magnitude of OS benefit was enriched compared with the overall population treated with nivolumab-plus-chemotherapy versus chemotherapy (HR 0.34, 95% CI 0.16–0.74; Fig. 2b), although sample sizes were small; patients with microsatellite stable (MSS) tumors had OS benefit similar to that of the overall population (MSS, HR 0.79, 95% CI 0.71–0.89; Fig. 2b; overall population, HR 0.69, 95% CI 0.60–0.79)[5].

Patients with TMB-high tumors seemed to benefit from nivolumab-plus-ipilimumab (HR 0.31, 95% CI 0.10–0.95), although the sample size in the TMB-high group was small (Fig. 2c); similar results were also observed in patients with PD-L1 CPS ≥ 5 (Extended Data Fig. 2b). In patients with MSI-high tumors, OS benefit was observed with nivolumab-plus-ipilimumab versus chemotherapy (HR 0.28, 95% CI 0.08–0.92) (Fig. 2d). OS results in patients with MSS tumors (HR 0.95, 95% CI 0.81–1.11) were consistent with the overall patient population[7] (Fig. 2d).

OS by genetic alterations

To characterize the impact of alterations in gastroesophageal adenocarcinoma-relevant genes, association of genetic changes (mutations or copy number) with OS was evaluated (Extended Data Fig. 3a and Supplementary Table 3). The most frequently altered genes among patients were *TP53* (55%), *ARID1A* (13%) and *KRAS*

Fig. 2 | OS by TMB in patients treated with nivolumab-plus-chemotherapy or nivolumab-plus-ipilimumab versus chemotherapy. a, Forest plot showing OS by baseline TMB status in patients who received nivolumab-plus-chemotherapy versus chemotherapy. Data are presented as unstratified HRs and 95% CI. **b**, Kaplan–Meier curves of OS by microsatellite stability status in patients treated with nivolumab-plus-chemotherapy versus chemotherapy. **c**, Forest plot showing OS by baseline TMB status in patients who received nivolumab-plus-ipilimumab versus chemotherapy. **d**, Kaplan–Meier curves of OS by microsatellite stability status in patients treated with nivolumab-plus-ipilimumab versus chemotherapy. TMB-high denotes ≥199 mutations per exome, whereas TMB-low denotes <199 mutations per exome. Data are presented as unstratified HRs and 95% CI. HR was not calculated if the number of patients in each arm was <5. [a]TMB not evaluable (NE)/available in 896 patients (NIVO + chemo: n = 431; Chemo: n = 465). [b]TMB not evaluable/available in 727 patients (NIVO + chemo: n = 355; Chemo: n = 372). [c]TMB not evaluable/available in 447 patients (NIVO + IPI: n = 226; Chemo: n = 221). [d]TMB not evaluable/available in 351 patients (NIVO + IPI: n = 181; Chemo: n = 170).

https://doi.org/10.1038/s41591-025-03575-0

a

Population	Status	Unstratified HR (95% CI)
All WES-evaluable	All evaluable[a] (*n* = 685)	0.80 (0.68–0.94)
	TMB-high (*n* = 57)	0.48 (0.25–0.91)
	TMB-low (*n* = 628)	0.85 (0.72–1.00)
All WES-evaluable (excluding MSI-H)	All evaluable[b] (*n* = 651)	0.82 (0.69–0.97)
	TMB-high (*n* = 26)	0.57 (0.21–1.51)
	TMB-low (*n* = 625)	0.84 (0.71–1.00)

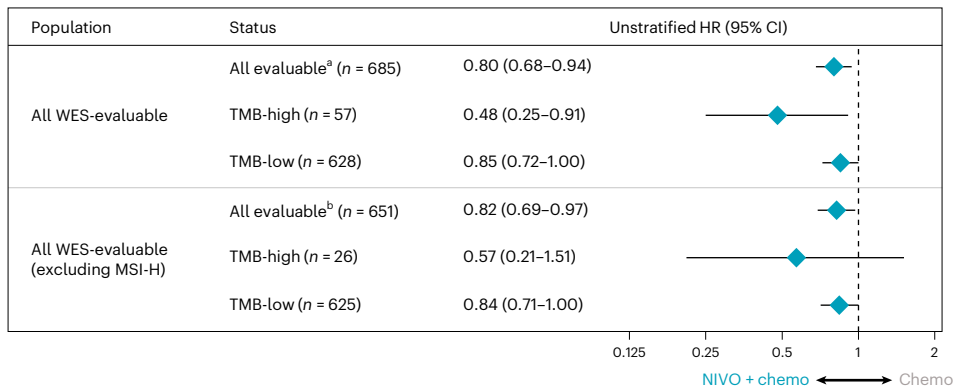

b

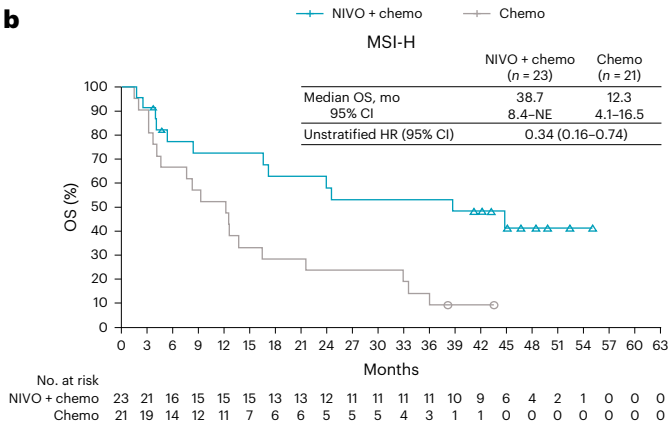

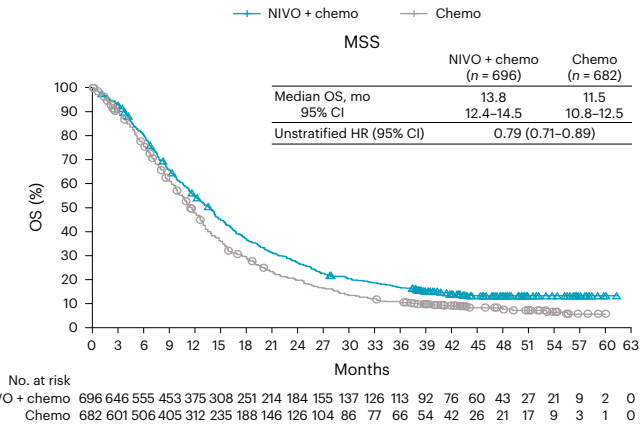

c

Population	Status	Unstratified HR (95% CI)
All WES-evaluable	All evaluable[c] (*n* = 366)	0.81 (0.65–1.00)
	TMB-high (*n* = 21)	0.31 (0.10–0.95)
	TMB-low (*n* = 345)	0.87 (0.70–1.09)
All WES-evaluable (excluding MSI-H)	All evaluable[d] (*n* = 348)	0.87 (0.70–1.08)
	TMB-high (*n* = 5)	N/A
	TMB-low (*n* = 343)	0.89 (0.71–1.11)

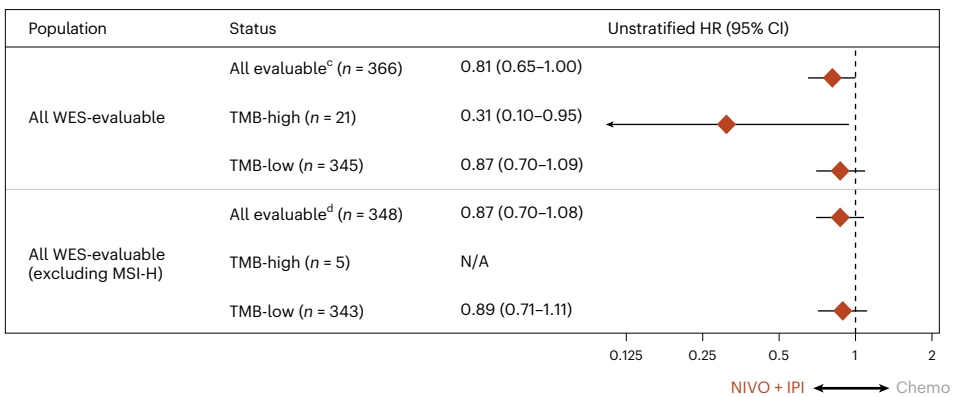

d

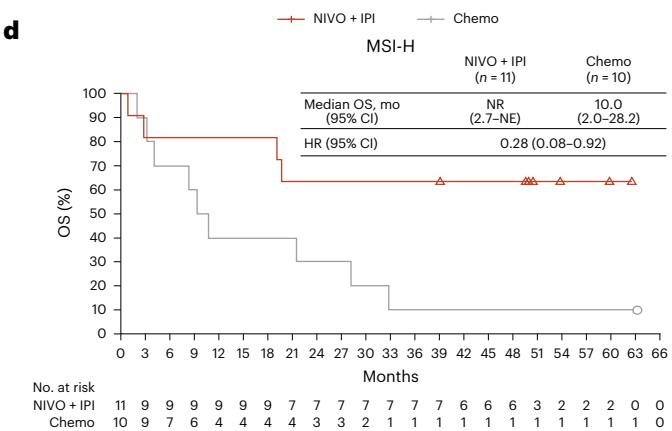

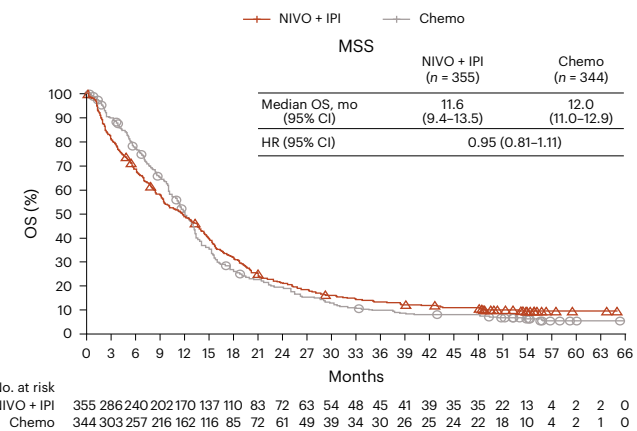

https://doi.org/10.1038/s41591-025-03575-0

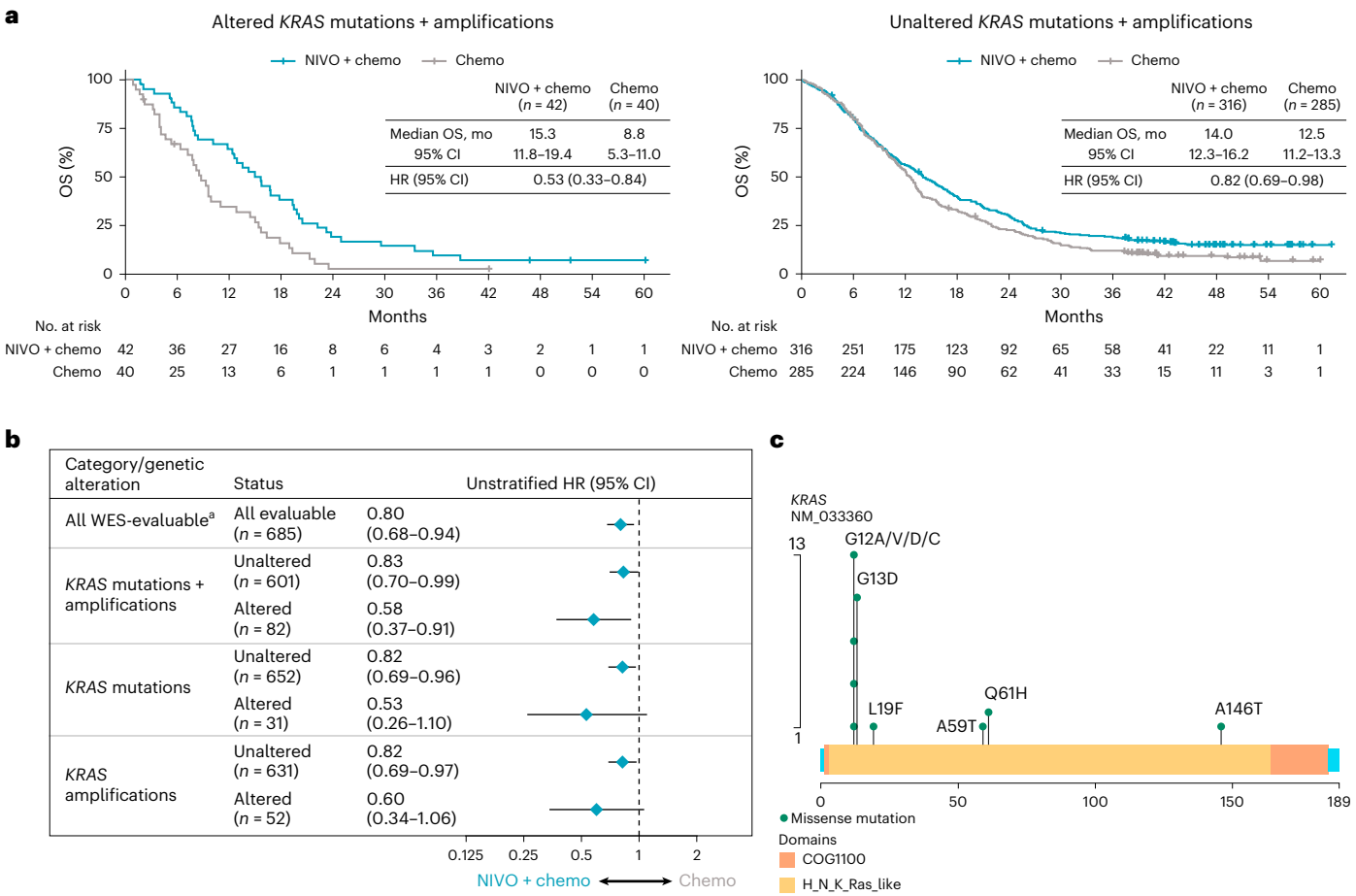

Fig. 3 | Efficacy by *KRAS* alterations in patients treated with nivolumab-plus-chemotherapy versus chemotherapy. a, Kaplan–Meier estimates of OS in all WES-evaluable patients with altered (left) or unaltered (right) *KRAS* mutations + amplifications. **b**, OS by baseline *KRAS* pathway alteration status derived from the model, including interaction of *KRAS* alteration status with treatment, MSI and TMB status. Data are presented as unstratified HRs and 95% CI. **c**, *KRAS* mutation map. [a]MSI status not evaluable/available in two patients. *KRAS*, Kirsten rat sarcoma viral oncogene.

(12%). The results suggest a general trend toward OS benefit with nivolumab-plus-chemotherapy versus chemotherapy across gene alteration subgroups; however, the interpretation is limited due to the small number of patients within each genomic subset, which led to wide confidence intervals (Extended Data Fig. 3b). Although benefit was observed regardless of *KRAS* alteration status, a higher magnitude of benefit was noted within the *KRAS*-altered subgroup (HR 0.53; Fig. 3a). Similar trends were observed when *KRAS* alterations were further categorized as mutations or amplifications; 31 patients (5%) had *KRAS* mutations, and 52 patients (8%) had *KRAS* amplifications (Fig. 3b). Most *KRAS* mutations seemed to occur at the G12 and G13 codons (Fig. 3c). Gene alterations did not have a notable impact on OS with nivolumab-plus-ipilimumab versus chemotherapy (Extended Data Fig. 3c), although patient numbers were small within some subgroups.

OS by GES

Baseline tumor GES of potential clinically and biologically relevant pathways spanning intrinsic and extrinsic tumor microenvironment factors (Supplementary Table 4) were evaluated for correlation with each other and separated into three modules: MAPK/hypoxia/glycolysis/proliferation, inflammation and angiogenesis/stroma. Inflammation-related GES including regulatory T (T_{reg}) cells showed moderate-to-strong correlation with each other (Fig. 4a). In the MAPK/hypoxia/glycolysis/proliferation module, the 34-gene MAPK GES was highly correlated with proliferation (Spearman's correlation $\rho = 0.9$), hypoxia (Spearman's correlation $\rho \geq 0.5$) and glycolysis-related GES (Spearman's correlation $\rho = 0.7$) (Fig. 4a). These observations were recapitulated when patients were clustered based on the same signatures, and grouped into three clusters, similar to the three modules in Fig. 4a. Tumors tended to have similar expression patterns of different signatures within the same cluster. CIN tumors tended to be enriched in patients with higher expression of MAPK/hypoxia/glycolysis/proliferation-related GES, and PD-L1 CPS ≥ 5 tumors were more frequently observed in patients with higher inflammation-related GES (Fig. 4b).

Several GES were associated with OS benefit from nivolumab-plus-chemotherapy versus chemotherapy ($P < 0.1$; likelihood ratio test (LRT)) (Extended Data Fig. 4a). This included multiple angiogenesis-, MAPK- and stroma-related signatures (Extended Data Fig. 4a). Further stratification of all RNA-seq-evaluable patients into tertiles based on GES high, medium or low scores was performed, and the results were visualized using Kaplan–Meier curves and forest plots (Fig. 5 and Extended Data Fig. 5). Low angiogenesis GES scores were associated with improved OS benefit in all-evaluable patients and those with PD-L1 CPS ≥ 5 or CPS < 5 (five-gene angiogenesis (low), all-evaluable, HR 0.68; CPS ≥ 5, HR 0.62; CPS < 5, HR 0.66; Fig. 5a,b and Extended Data Fig. 5b,c). Low stroma and high MAPK GES scores were also associated with improved OS with nivolumab-plus-chemotherapy versus chemotherapy in the all-evaluable and PD-L1 CPS ≥ 5 subgroups (Fig. 5a and Extended Data Fig. 5b). No obvious associations of OS benefit with inflammatory GES were observed.

Associations were also observed between GES and OS benefit in the nivolumab-plus-ipilimumab versus chemotherapy group ($P < 0.1$; LRT);

https://doi.org/10.1038/s41591-025-03575-0

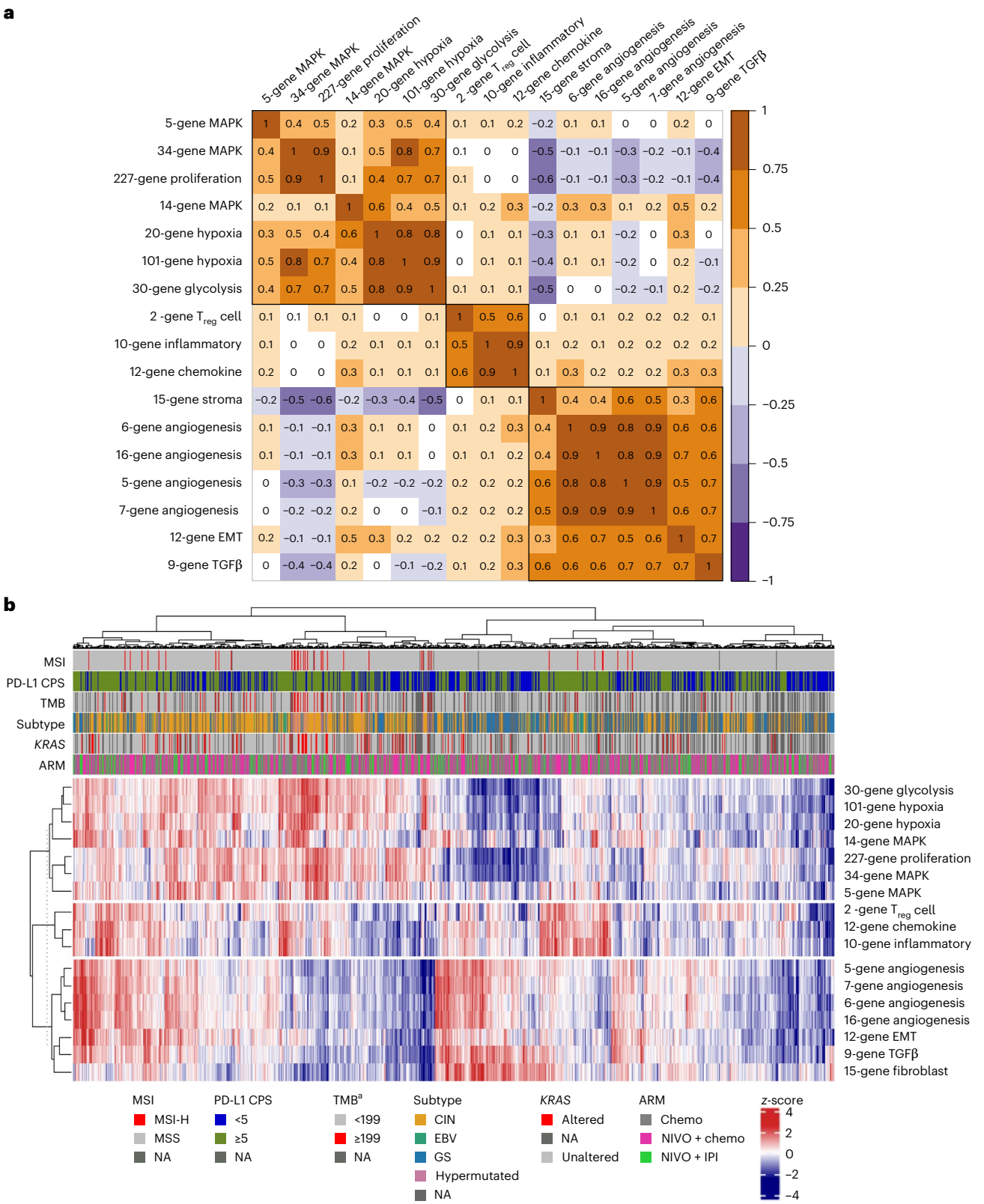

Fig. 4 | Relationship between key biomarkers in all patients treated with nivolumab-plus-chemotherapy, nivolumab-plus-ipilimumab or chemotherapy. a, Correlation of gene signatures among all RNA-seq evaluable patients. Numbers indicate the Spearman's correlation. The strength of association is indicated by the color scale shown on the right. **b**, Heatmap of baseline tumors clustered by the gene signatures of interest in patients treated with nivolumab-plus-chemotherapy, nivolumab-plus-ipilimumab or chemotherapy. For visualization purposes, each gene signature was first normalized by *z*-score method where samples with high *z*-score (red) indicates relative high gene signature score and low *z*-score (blue) indicates relative low gene signature score. Patients (column) were ordered based on similarity of gene signatures of their tumor samples via hierarchical clustering method. Dendrogram (top) was added to show the hierarchical relationship between samples. Similarly, gene signatures (rows) were ordered and dendrogram (left) was added to show the hierarchical relationship between gene signatures. [a]Mutations per exome.

https://doi.org/10.1038/s41591-025-03575-0

a

Category/GES	Status	Unstratified HR (95% CI)
All evaluable	(*n* = 809)	0.78 (0.67–0.90)
5-gene angiogenesis	High (*n* = 270)	0.89 (0.68–1.15)
	Medium (*n* = 269)	0.78 (0.60–1.01)
	Low (*n* = 270)	0.68 (0.52–0.88)
15-gene stroma	High (*n* = 270)	0.97 (0.75–1.25)
	Medium (*n* = 269)	0.71 (0.55–0.92)
	Low (*n* = 270)	0.69 (0.53–0.89)
5-gene MAPK	High (*n* = 270)	0.64 (0.50–0.83)
	Medium (*n* = 269)	0.78 (0.60–1.02)
	Low (*n* = 270)	0.99 (0.77–1.27)

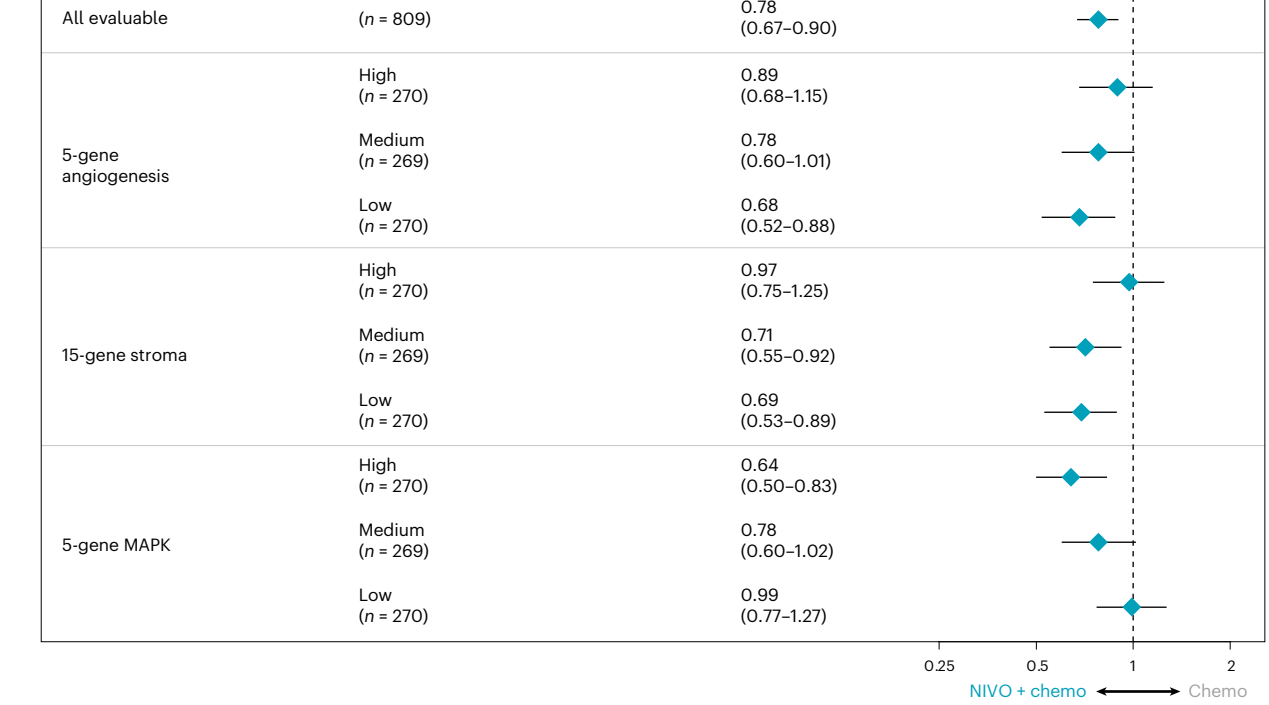

b

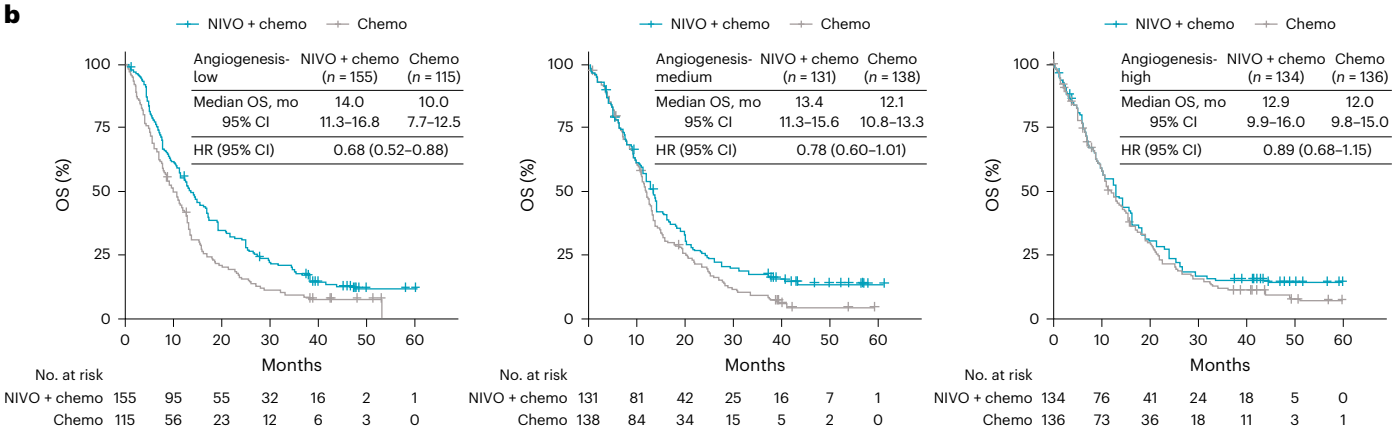

Fig. 5 | OS by GES scores in patients treated with nivolumab-plus-chemotherapy versus chemotherapy. a, Forest plot showing the correlation between OS and selected signatures used to stratify patients into tertiles (high, medium or low). Data are presented as unstratified HRs and 95% CI. HR was not calculated if the number of patients in each arm was <5. **b**, Kaplan–Meier estimates of OS in all RNA-seq-evaluable patients with low, medium or high angiogenesis GES scores (five-gene angiogenesis) at baseline.

these GES included angiogenesis-, glycolysis-, hypoxia-, inflammatory-, chemokine-, T_{reg} cell-, MAPK-, proliferation- and stroma-related signatures (Extended Data Fig. 4b). Numerous GES subgroups by tertiles showed OS benefit with nivolumab-plus-ipilimumab versus chemotherapy (Fig. 6). OS benefit was observed in patients with high inflammation GES scores among all-evaluable patients (12-gene chemokine (high), HR, 0.59; ten-gene inflammation (high), HR 0.63; Fig. 5) and those with PD-L1 CPS ≥ 5 (HR 0.77; Extended Data Fig. 6). Improved OS was also observed in patients with high T_{reg} GES score regardless of PD-L1 status (two-gene T_{reg} cell (high), all-evaluable, HR 0.59; PD-L1 CPS ≥ 5, HR 0.57; PD-L1 CPS < 5, HR 0.51); the Kaplan–Meier OS curves for these subgroups demonstrated no evidence of an early detriment with nivolumab-plus-ipilimumab versus chemotherapy (Fig. 5a,b and Extended Data Fig. 7). Multivariate analysis adjusting for baseline inflammation demonstrated a similar association of high T_{reg} cell GES scores with OS benefit for nivolumab-plus-ipilimumab versus chemotherapy, suggesting that this effect was not driven by baseline inflammation levels (T_{reg} cell (high) adjusted by ten-gene inflammation, all-evaluable, HR 0.57 (95% CI 0.39–0.83); PD-L1 CPS ≥ 5, HR 0.57 (95% CI 0.35–0.92); PD-L1 CPS < 5, HR 0.46 (95% CI 0.24–0.86)). A summary of the various GES potentially associated with efficacy with nivolumab-plus-chemotherapy or nivolumab-plus-ipilimumab is provided in Extended Data Fig. 8.

To further explore associations of GES with efficacy of nivolumab-plus-chemotherapy or nivolumab-plus-ipilimumab, gene set enrichment analysis (GSEA) was conducted (Extended Data Fig. 9). Enrichment of inflammation-related gene sets (interferon_alpha_response and allograft_rejection)[32,33] were prognostic for OS benefit in both nivolumab-plus-chemotherapy and chemotherapy (false discovery rate <0.01); however, these were predictive of better OS benefit with

https://doi.org/10.1038/s41591-025-03575-0

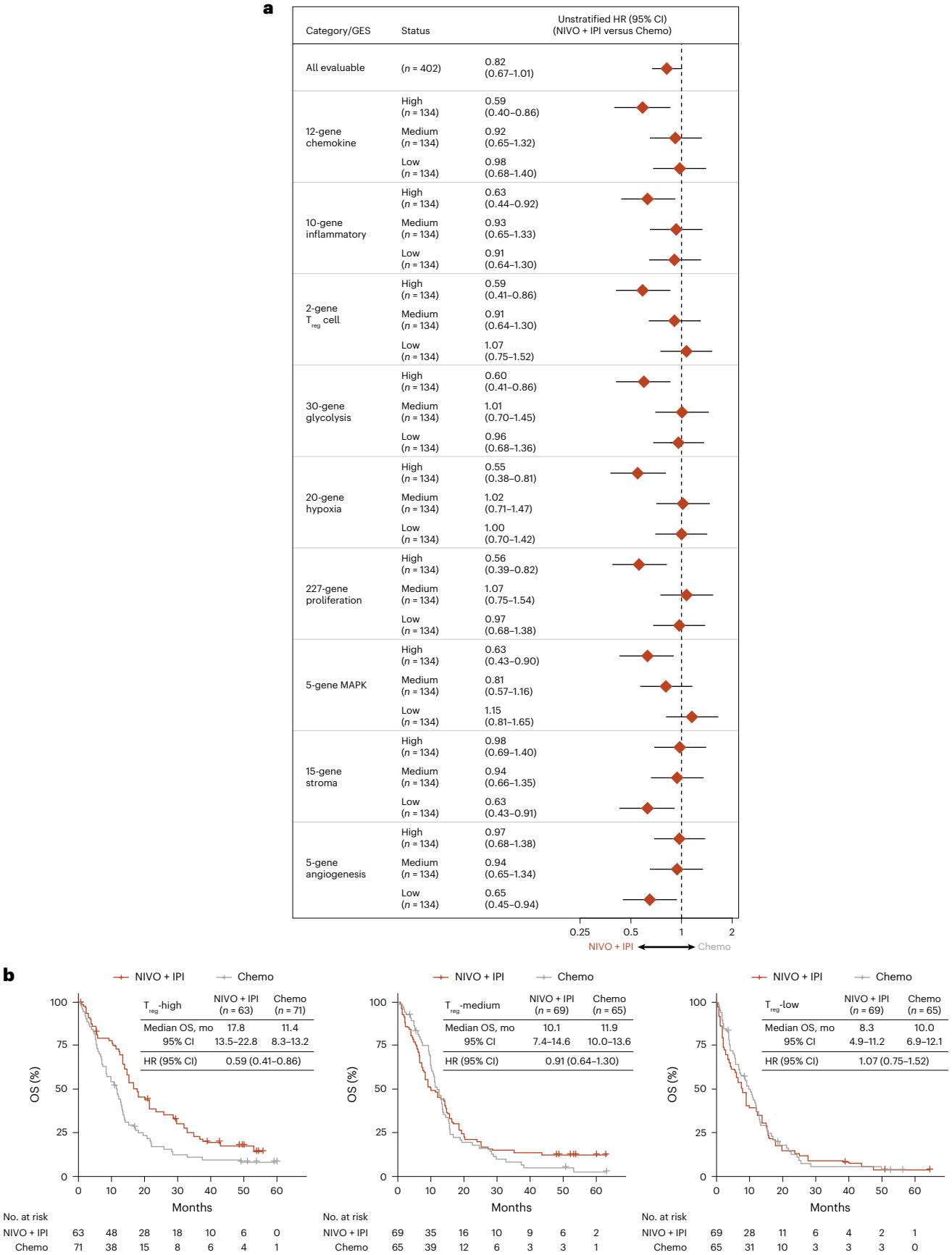

Fig. 6 | OS by GES scores in patients treated with nivolumab-plus-ipilimumab versus chemotherapy. a, Forest plot showing the correlation between OS and selected signatures used to stratify patients into tertiles (high, medium or low). Data are presented as unstratified HRs and 95% CI. HR was not calculated if the number of patients in each arm was <5. **b**, Kaplan–Meier estimates of OS in all RNA-seq-evaluable patients with high, medium or low T_{reg} cell GES scores (two-gene T_{reg} cell) at baseline.

nivolumab-plus-ipilimumab versus chemotherapy (Extended Data Fig. 9). Cell cycle-related gene sets (MYC_targets_v1, G2M_checkpoint and E2F_targets) were enriched with genes predictive of better OS with both nivolumab-plus-chemotherapy or nivolumab-plus-ipilimumab versus chemotherapy (Extended Data Fig. 9). The epithelial–mesenchymal transition gene set was prognostic of worse OS in all three treatment groups (adjusted *P* value of interaction >0.9; Extended Data Fig. 9).

Discussion

This analysis from the CheckMate 649 study utilized large-scale WES and RNA-seq analyses to gain deeper understanding of signaling pathways associated with favorable outcomes with nivolumab-plus-chemotherapy or nivolumab-plus-ipilimumab versus chemotherapy. To our knowledge, this study provides the largest WES and RNA-seq datasets with first-line immune checkpoint blockade in gastroesophageal adenocarcinoma.

Genomic subtyping analyses of all WES-evaluable tumors from CheckMate 649 showed that the CIN subtype was predominant in esophageal and gastroesophageal junction adenocarcinomas. In WES-evaluable patients, differential associations of OS benefit with genomic subtypes were observed for nivolumab-plus-chemotherapy and nivolumab-plus-ipilimumab versus chemotherapy. Greater OS benefit was observed with nivolumab-plus-chemotherapy and with nivolumab-plus-ipilimumab versus chemotherapy among patients with the hypermutated subtype, followed by EBV; however, the small sample size in this subgroup limits interpretation.

Several studies have shown that CIN is linked to cancer progression and metastasis due to increased cancer cell migration and immune evasion[34–36]. One of the CIN-driven mechanisms to evade the immune system is the chronic activation of the cGAS–STING pathway, which increases resistance to anti-PD-1/PD-L1 treatment[35–37]. In CheckMate 649, adding ipilimumab to nivolumab may have potentially reduced the effect of this immune evasion in CIN tumors, leading to OS benefit, although further confirmation is required. Novel therapeutic options and combination strategies may be needed to further improve outcomes in patients with CIN tumors.

OS benefit with nivolumab-plus-chemotherapy versus chemotherapy was generally observed regardless of gene alteration status; alterations in *TP53*, *ARID1A* and *KRAS* were the most common in these analyses. Notably, patients with tumors harboring *KRAS* alterations derived a higher magnitude of benefit with nivolumab-plus-chemotherapy versus chemotherapy compared with the *KRAS*-unaltered subgroup. Although definitive conclusions cannot be drawn from these findings due to small patient numbers in some subgroups, similar results were reported in lung cancer studies, where there were better outcomes with immunotherapy-based regimens than with chemotherapy-based regimens[38–40]. The underlying mechanisms for the improved efficacy with nivolumab-plus-chemotherapy in gastric tumors with *KRAS* alterations are yet to be established. However, several studies previously demonstrated that mutant KRAS promotes an immunosuppressive tumor microenvironment through multiple mechanisms, such as increased release of IL-10 and TGF-β via the ERK–MAPK pathway, resulting in promotion of T_{reg} cells and inhibition of $CD8^+$ T cell activity[41,42]. Blocking PD-1 can counteract these effects by reinvigorating $CD8^+$ T cell responses and reducing the immunosuppressive impact of mutant KRAS on the tumor microenvironment, leading to potentially better outcomes in *KRAS*-mutant cancers under immune checkpoint inhibition. In addition, oncogenic KRAS signaling is capable of upregulating noncoding transcripts arising from transposable elements, which are known to increase tumor immunogenicity[43]. These factors may lead to an increased susceptibility to immunotherapies.

TMB is lower in gastroesophageal cancers compared with lung cancer and melanoma[44]. Consistent with these data, 8% of patients evaluable for this biomarker had TMB-high tumors in this study; all TMB-high tumors were also MSI-high. Nevertheless, a trend toward improved OS benefit with nivolumab-plus-chemotherapy or nivolumab-plus-ipilimumab versus chemotherapy was observed among patients with high TMB, in both all-randomized and PD-L1 CPS ≥ 5 populations. Similar results have been reported in other tumor types following treatment with immune checkpoint inhibitors[22–26,45]; however, this relationship could not be evaluated in patients with high TMB and PD-L1 CPS < 5 due to small sample size.

In RNA-seq analyses, subgroups with low angiogenesis and low stroma GES scores were associated with greater OS benefit with nivolumab-plus-chemotherapy and nivolumab-plus-ipilimumab versus chemotherapy. Notably, low angiogenesis GES scores were associated with OS benefit of nivolumab-plus-chemotherapy versus chemotherapy even in the PD-L1 CPS < 5 subgroup. These findings are aligned with the known interplay of angiogenesis and stromal/fibroblast signaling that leads to immune suppression and resistance to immune checkpoint blockade, likely through impaired vasculature and stromal aberrations resulting in reduced perfusion limiting the entry and function of effector T cells into the tumor microenvironment[46–49]. Furthermore, vascular endothelial growth factor (VEGF), which plays a critical role in angiogenesis, activates and recruits immune suppressive cells such as T_{reg} cells and tumor-associated macrophages[50]. The combination of immunotherapy and anti-angiogenic/anti-fibroblast agents may potentially overcome tumor resistance to anticancer agents and improve treatment outcomes in gastroesophageal cancer[51–59]. Tumor T cell inflammation is a known predictive biomarker for immune checkpoint blockade in gastroesophageal and other tumor types[29,60,61]. Notably, although our analyses indicated an association between baseline inflammation and efficacy of nivolumab-plus-ipilimumab, the trend was less obvious with nivolumab-plus-chemotherapy. This may be due to activation of proinflammatory signaling following chemotherapy-induced cytotoxicity and immunogenic cell death resulting in reduced dependence of nivolumab-plus-chemotherapy antitumor activity on baseline inflammation[16,62].

High numbers of tumor-infiltrating T_{reg} cells are correlated with poor prognosis in gastric cancer and other tumor types[63–66] and with possible resistance to PD-1 inhibitor therapy[67,68]. In the current analysis, high T_{reg} cell GES scores emerged as unique signatures associated with OS benefit from nivolumab-plus-ipilimumab versus chemotherapy regardless of PD-L1 CPS status. The association of high T_{reg} cell GES scores with OS benefit was still observed when adjusted for baseline inflammation, despite the known correlation between T_{reg} cell GES and inflammation. This may be attributed to ipilimumab-driven T_{reg} cell modulation, enhanced ratio of effector T to T_{reg} cells and $CD4^+$ T cell activation[69]. Further studies are needed to confirm the mechanistic interaction of ipilimumab with effector T and T_{reg} cells in gastroesophageal adenocarcinoma. Proliferation GES are known to be associated with better response to immunotherapy[70,71], and high proliferation was associated with OS benefit with nivolumab-plus-ipilimumab versus chemotherapy in our analysis. Glycolysis and hypoxia GES, which showed moderate-to-strong correlation with proliferation GES, were also associated with potential benefit of nivolumab-plus-ipilimumab versus chemotherapy. The results from GSEA were largely consistent with RNA-seq data, supporting the robustness of this analysis. Of note, cell cycle-related gene sets, which correlate with cell cycle progression and MAPK pathway activation, were predictive of better OS with both nivolumab-plus-chemotherapy and nivolumab-plus-ipilimumab versus chemotherapy, consistent with the GES analysis that demonstrated the association between MAPK GES and OS benefit for both nivolumab-based regimens. Interestingly, *KRAS* alteration was associated with higher OS benefit in patients treated with nivolumab-plus-chemotherapy but not nivolumab-plus-ipilimumab versus chemotherapy, indicating that MAPK pathway influence on cancer outcome is not dictated by *KRAS* alteration status. The minor differences observed between RNA-seq and GSEA may be due to some

variations in the genes between the hallmark gene sets used in the GSEA and those that comprised the GES.

The current analyses have some limitations. Although the biomarker-evaluable populations were generally representative of the all-randomized study population with respect to demographics, baseline clinical characteristics and outcomes, the small sample sizes of each biomarker subgroup may have resulted in imbalances that are not captured by these measurements. Additionally, these retrospective biomarker analyses were exploratory and therefore were not formally tested or intended to determine statistical significance. Thus, the utility of these biomarkers requires further prospective clinical validation.

This exploratory biomarker analysis from the CheckMate 649 study identified patient populations with gastric, gastroesophageal junction and esophageal adenocarcinoma that seem to derive greater OS benefit from first-line nivolumab-plus-chemotherapy or potential benefit from nivolumab-plus-ipilimumab versus chemotherapy. The pattern of biomarkers identified in this analysis suggests a role for overlapping (anti-PD-1) and distinct (anti-CTLA-4) mechanisms from these immunotherapy regimens. Additional prospective clinical studies are needed to determine if these predictive biomarkers hold clinical utility for treatment selection.

Online content

Any methods, additional references, Nature Portfolio reporting summaries, source data, extended data, supplementary information, acknowledgements, peer review information; details of author contributions and competing interests; and statements of data and code availability are available at https://doi.org/10.1038/s41591-025-03575-0.

References

1. Lordick, F. et al. Capecitabine and cisplatin with or without cetuximab for patients with previously untreated advanced gastric cancer (EXPAND): a randomised, open-label phase 3 trial. *Lancet Oncol.* **14**, 490–499 (2013).
2. Catenacci, D. V. T. et al. Rilotumumab plus epirubicin, cisplatin, and capecitabine as first-line therapy in advanced MET-positive gastric or gastro-oesophageal junction cancer (RILOMET-1): a randomised, double-blind, placebo-controlled, phase 3 trial. *Lancet Oncol.* **18**, 1467–1482 (2017).
3. Shah, M. A. et al. Effect of fluorouracil, leucovorin, and oxaliplatin with or without onartuzumab in HER2-negative, MET-positive gastroesophageal adenocarcinoma: the METGastric randomized clinical trial. *JAMA Oncol.* **3**, 620–627 (2017).
4. Fuchs, C. S. et al. Ramucirumab with cisplatin and fluoropyrimidine as first-line therapy in patients with metastatic gastric or junctional adenocarcinoma (RAINFALL): a double-blind, randomised, placebo-controlled, phase 3 trial. *Lancet Oncol.* **20**, 420–435 (2019).
5. Janjigian, Y. Y. et al. First-line nivolumab plus chemotherapy versus chemotherapy alone for advanced gastric, gastro-oesophageal junction, and oesophageal adenocarcinoma (CheckMate 649): a randomised, open-label, phase 3 trial. *Lancet* **398**, 27–40 (2021).
6. Bristol Myers Squibb. OPDIVO (nivolumab prescribing information) (Bristol Myers Squibb, 2024); https://packageinserts.bms.com/pi/pi_opdivo.pdf
7. Shitara, K. et al. Nivolumab plus chemotherapy or ipilimumab in gastro-oesophageal cancer. *Nature* **603**, 942–948 (2022).
8. Curran, M. A., Montalvo, W., Yagita, H. & Allison, J. P. PD-1 and CTLA-4 combination blockade expands infiltrating T cells and reduces regulatory T and myeloid cells within B16 melanoma tumors. *Proc. Natl Acad. Sci. USA* **107**, 4275–4280 (2010).
9. Das, R. et al. Combination therapy with anti-CTLA-4 and anti-PD-1 leads to distinct immunologic changes in vivo. *J. Immunol.* **194**, 950–959 (2015).
10. Wang, C. et al. In vitro characterization of the anti-PD-1 antibody nivolumab, BMS-936558, and in vivo toxicology in non-human primates. *Cancer Immunol. Res.* **2**, 846–856 (2014).
11. Pardoll, D. M. The blockade of immune checkpoints in cancer immunotherapy. *Nat. Rev. Cancer* **12**, 252–264 (2012).
12. Wei, S. C., Duffy, C. R. & Allison, J. P. Fundamental mechanisms of immune checkpoint blockade therapy. *Cancer Discov.* **8**, 1069–1086 (2018).
13. Yofe, I. et al. Anti-CTLA-4 antibodies drive myeloid activation and reprogram the tumor microenvironment through FcγR engagement and type I interferon signaling. *Nat. Cancer* **3**, 1336–1350 (2022).
14. Zappasodi, R. et al. CTLA-4 blockade drives loss of Treg stability in glycolysis-low tumours. *Nature* **591**, 652–658 (2021).
15. Wei, S. C. et al. Combination anti-CTLA-4 plus anti-PD-1 checkpoint blockade utilizes cellular mechanisms partially distinct from monotherapies. *Proc. Natl Acad. Sci. USA* **116**, 22699–22709 (2019).
16. Salas-Benito, D. et al. Paradigms on immunotherapy combinations with chemotherapy. *Cancer Discov.* **11**, 1353–1367 (2021).
17. Cancer Genome Atlas Research Network. Comprehensive molecular characterization of gastric adenocarcinoma. *Nature* **513**, 202–209 (2014).
18. Xie, T. et al. Positive status of Epstein–Barr virus as a biomarker for gastric cancer immunotherapy: a prospective observational study. *J. Immunother.* **43**, 139–144 (2020).
19. Maio, M. et al. Pembrolizumab in microsatellite instability high or mismatch repair deficient cancers: updated analysis from the phase II KEYNOTE-158 study. *Ann. Oncol.* **33**, 929–938 (2022).
20. Fuchs, C. S. et al. Safety and efficacy of pembrolizumab monotherapy in patients with previously treated advanced gastric and gastroesophageal junction cancer: phase 2 clinical KEYNOTE-059 trial. *JAMA Oncol.* **4**, e180013 (2018).
21. Shitara, K. et al. Molecular determinants of clinical outcomes with pembrolizumab versus paclitaxel in a randomized, open-label, phase III trial in patients with gastroesophageal adenocarcinoma. *Ann. Oncol.* **32**, 1127–1136 (2021).
22. Hellmann, M. D. et al. Genomic features of response to combination immunotherapy in patients with advanced non-small-cell lung cancer. *Cancer Cell* **33**, 843–852.e844 (2018).
23. Rosenberg, J. E. et al. Atezolizumab in patients with locally advanced and metastatic urothelial carcinoma who have progressed following treatment with platinum-based chemotherapy: a single-arm, multicentre, phase 2 trial. *Lancet* **387**, 1909–1920 (2016).
24. Snyder, A. et al. Genetic basis for clinical response to CTLA-4 blockade in melanoma. *N. Engl. J. Med.* **371**, 2189–2199 (2014).
25. Van Allen, E. M. et al. Genomic correlates of response to CTLA-4 blockade in metastatic melanoma. *Science* **350**, 207–211 (2015).
26. Johnson, D. B. et al. Targeted next generation sequencing identifies markers of response to PD-1 blockade. *Cancer Immunol. Res.* **4**, 959–967 (2016).
27. Marabelle, A. et al. Association of tumour mutational burden with outcomes in patients with advanced solid tumours treated with pembrolizumab: prospective biomarker analysis of the multicohort, open-label, phase 2 KEYNOTE-158 study. *Lancet Oncol.* **21**, 1353–1365 (2020).
28. Cristescu, R. et al. Tumor mutational burden predicts the efficacy of pembrolizumab monotherapy: a pan-tumor retrospective analysis of participants with advanced solid tumors. *J. Immunother. Cancer* **10**, e003091 (2022).
29. Lei, M. et al. Analyses of PD-L1 and inflammatory gene expression association with efficacy of nivolumab ± ipilimumab in gastric cancer/gastroesophageal junction cancer. *Clin. Cancer Res.* **27**, 3926–3935 (2021).

30. Shiuan, E. et al. Clinical features and multiplatform molecular analysis assist in understanding patient response to anti-PD-1/PD-L1 in renal cell carcinoma. *Cancers* **13**, 1475 (2021).
31. Wang, L. et al. EMT- and stroma-related gene expression and resistance to PD-1 blockade in urothelial cancer. *Nat. Commun.* **9**, 3503 (2018).
32. Mootha, V. K. et al. PGC-1α-responsive genes involved in oxidative phosphorylation are coordinately downregulated in human diabetes. *Nat. Genet.* **34**, 267–273 (2003).
33. Subramanian, A. et al. Gene set enrichment analysis: a knowledge-based approach for interpreting genome-wide expression profiles. *Proc. Natl Acad. Sci. USA* **102**, 15545–15550 (2005).
34. Davoli, T., Uno, H., Wooten, E. C. & Elledge, S. J. Tumor aneuploidy correlates with markers of immune evasion and with reduced response to immunotherapy. *Science* **355**, eaaf8399 (2017).
35. Bakhoum, S. F. et al. Chromosomal instability drives metastasis through a cytosolic DNA response. *Nature* **553**, 467–472 (2018).
36. Li, J. et al. Non-cell-autonomous cancer progression from chromosomal instability. *Nature* **620**, 1080–1088 (2023).
37. Li, J. et al. Metastasis and immune evasion from extracellular cGAMP hydrolysis. *Cancer Discov.* **11**, 1212–1227 (2021).
38. Huang, L., Guo, Z., Wang, F. & Fu, L. KRAS mutation: from undruggable to druggable in cancer. *Signal Transduct. Target Ther.* **6**, 386 (2021).
39. Sun, L. et al. Association between KRAS variant status and outcomes with first-line immune checkpoint inhibitor-based therapy in patients with advanced non-small-cell lung cancer. *JAMA Oncol.* **7**, 937–939 (2021).
40. Peng, L. et al. Efficacy of immunotherapy in KRAS-mutant advanced NSCLC: a real-world study in a Chinese population. *Front. Oncol.* **12**, 1070761 (2022).
41. Batlle, E. & Massagué, J. Transforming growth factor-β signaling in immunity and cancer. *Immunity* **50**, 924–940 (2019).
42. Molina-Arcas, M. & Downward, J. Exploiting the therapeutic implications of KRAS inhibition on tumor immunity. *Cancer Cell* **42**, 338–357 (2024).
43. Reggiardo, R. E. et al. Mutant KRAS regulates transposable element RNA and innate immunity via KRAB zinc-finger genes. *Cell Rep.* **40**, 111104 (2022).
44. Sivakumar, S. et al. Tumor mutational burden reveals tumor-specific patterns with intra-patient stability from multiple longitudinal tissue biopsies from 3,402 patients. *Cancer Res.* https://doi.org/10.1158/1538-7445.AM2021-472 (2021).
45. Rizvi, N. A. et al. Cancer immunology. Mutational landscape determines sensitivity to PD-1 blockade in non-small cell lung cancer. *Science* **348**, 124–128 (2015).
46. Brown, J. M. Tumor hypoxia in cancer therapy. *Methods Enzymol.* **435**, 297–321 (2007).
47. Yuan, F. et al. Microvascular permeability and interstitial penetration of sterically stabilized (stealth) liposomes in a human tumor xenograft. *Cancer Res.* **54**, 3352–3356 (1994).
48. Rahma, O. E. & Hodi, F. S. The intersection between tumor angiogenesis and immune suppression. *Clin. Cancer Res.* **25**, 5449–5457 (2019).
49. Jain, R. K. Normalizing tumor microenvironment to treat cancer: bench to bedside to biomarkers. *J. Clin. Oncol.* **31**, 2205–2218 (2013).
50. Ribatti, D. Immunosuppressive effects of vascular endothelial growth factor (review). *Oncol Lett.* **24**, 369 (2022).
51. Schmittnaegel, M. et al. Dual angiopoietin-2 and VEGFA inhibition elicits antitumor immunity that is enhanced by PD-1 checkpoint blockade. *Sci. Transl. Med.* **9**, eaak9670 (2017).
52. Yasuda, S. et al. Simultaneous blockade of programmed death 1 and vascular endothelial growth factor receptor 2 (VEGFR2) induces synergistic anti-tumour effect in vivo. *Clin. Exp. Immunol.* **172**, 500–506 (2013).
53. Voron, T. et al. VEGF-A modulates expression of inhibitory checkpoints on $CD8^+$ T cells in tumors. *J. Exp. Med.* **212**, 139–148 (2015).
54. Allen, E. et al. Combined antiangiogenic and anti-PD-L1 therapy stimulates tumor immunity through HEV formation. *Sci. Transl. Med.* **9**, eaak9679 (2017).
55. Wu, F. T. et al. Efficacy of cotargeting angiopoietin-2 and the VEGF pathway in the adjuvant postsurgical setting for early breast, colorectal, and renal cancers. *Cancer Res.* **76**, 6988–7000 (2016).
56. Fukumura, D. et al. Tumor induction of VEGF promoter activity in stromal cells. *Cell* **94**, 715–725 (1998).
57. Cytryn, S. L. et al. First-line regorafenib with nivolumab and chemotherapy in advanced oesophageal, gastric, or gastro-oesophageal junction cancer in the USA: a single-arm, single-centre, phase 2 trial. *Lancet Oncol.* **24**, 1073–1082 (2023).
58. Fukuoka, S. et al. Regorafenib plus nivolumab in patients with advanced gastric or colorectal cancer: an open-label, dose-escalation, and dose-expansion phase Ib trial (REGONIVO, EPOC1603). *J. Clin. Oncol.* **38**, 2053–2061 (2020).
59. Kawazoe, A. et al. Lenvatinib plus pembrolizumab in patients with advanced gastric cancer in the first-line or second-line setting (EPOC1706): an open-label, single-arm, phase 2 trial. *Lancet Oncol.* **21**, 1057–1065 (2020).
60. Hodi, F. S. et al. TMB and inflammatory gene expression associated with clinical outcomes following immunotherapy in advanced melanoma. *Cancer Immunol. Res.* **9**, 1202–1213 (2021).
61. Sangro, B. et al. Association of inflammatory biomarkers with clinical outcomes in nivolumab-treated patients with advanced hepatocellular carcinoma. *J. Hepatol.* **73**, 1460–1469 (2020).
62. Ahmed, A. & Tait, S. W. G. Targeting immunogenic cell death in cancer. *Mol. Oncol.* **14**, 2994–3006 (2020).
63. Bates, G. J. et al. Quantification of regulatory T cells enables the identification of high-risk breast cancer patients and those at risk of late relapse. *J. Clin. Oncol.* **24**, 5373–5380 (2006).
64. Sasada, T., Kimura, M., Yoshida, Y., Kanai, M. & Takabayashi, A. $CD4^+CD25^+$ regulatory T cells in patients with gastrointestinal malignancies: possible involvement of regulatory T cells in disease progression. *Cancer* **98**, 1089–1099 (2003).
65. Curiel, T. J. et al. Specific recruitment of regulatory T cells in ovarian carcinoma fosters immune privilege and predicts reduced survival. *Nat. Med.* **10**, 942–949 (2004).
66. Sato, E. et al. Intraepithelial $CD8^+$ tumor-infiltrating lymphocytes and a high $CD8^+$/regulatory T cell ratio are associated with favorable prognosis in ovarian cancer. *Proc. Natl Acad. Sci. USA* **102**, 18538–18543 (2005).
67. Kumagai, S. et al. The PD-1 expression balance between effector and regulatory T cells predicts the clinical efficacy of PD-1 blockade therapies. *Nat. Immunol.* **21**, 1346–1358 (2020).
68. Kamada, T. et al. PD-1(+) regulatory T cells amplified by PD-1 blockade promote hyperprogression of cancer. *Proc. Natl Acad. Sci. USA* **116**, 9999–10008 (2019).
69. Romano, E. et al. Ipilimumab-dependent cell-mediated cytotoxicity of regulatory T cells ex vivo by nonclassical monocytes in melanoma patients. *Proc. Natl Acad. Sci. USA* **112**, 6140–6145 (2015).
70. Pabla, S. et al. Integration of tumor inflammation, cell proliferation, and traditional biomarkers improves prediction of immunotherapy resistance and response. *Biomark. Res.* **9**, 56 (2021).
71. Pabla, S. et al. Proliferative potential and resistance to immune checkpoint blockade in lung cancer patients. *J. Immunother. Cancer* **7**, 27 (2019).

Kohei Shitara[1,2,26], Yelena Y. Janjigian[3,4,26] ✉, Jaffer Ajani[5], Markus Moehler[6], Jin Yao[7], Xuya Wang[7,23], Aparna Chhibber[7], Dimple Pandya[7,24], Lin Shen[8], Marcelo Garrido[9], Carlos Gallardo[10], Lucjan Wyrwicz[11], Kensei Yamaguchi[12], Tomasz Skoczylas[13], Arinilda Bragagnoli[14], Tianshu Liu[15], Michael Schenker[16], Patricio Yañez[17], Ruben Kowalyszyn[18], Michalis Karamouzis[19], Thomas Zander[20], Kynan Feeney[21], Elena Elimova[22], Parul Doshi[7,25], Mingshun Li[7] & Ming Lei[7] ✉

[1]National Cancer Center Hospital East, Kashiwa, Japan. [2]Department of Immunology, Nagoya University Graduate School of Medicine, Aichi, Japan. [3]Memorial Sloan Kettering Cancer Center, New York, NY, USA. [4]Weill Cornell Medical College, New York, NY, USA. [5]The University of Texas MD Anderson Cancer Center, Houston, TX, USA. [6]Johannes-Gutenberg University Clinic, Mainz, Germany. [7]Bristol Myers Squibb, Princeton, NJ, USA. [8]Peking University Cancer Hospital and Institute, Beijing, China. [9]Pontificia Universidad Católica-Universidad Mayor, Santiago, Chile. [10]Fundacion Arturo Lopez Perez, Providencia, Chile. [11]Narodowy Instytut Onkologii, Warsaw, Poland. [12]Cancer Institute Hospital of the Japanese Foundation for Cancer Research, Tokyo, Japan. [13]Medical University of Lublin, Lublin, Poland. [14]Fundaçao Pio XII - Hospital de Câncer de Barretos, Barretos, Brazil. [15]Zhongshan Hospital Fudan University, Shanghai, China. [16]Sfantul Nectarie Oncology Center, Dolj, Romania. [17]Universidad de La Frontera, Temuco, Chile. [18]Clinica Viedma SA, Viedma, Argentina. [19]National and Kapodistrian University of Athens, Athens, Greece. [20]University Hospital of Cologne, Cologne, Germany. [21]Notre Dame University and Edith Cowan University, Murdoch, Western Australia, Australia. [22]Princess Margaret Cancer Centre, Toronto, Ontario, Canada. [23]Present address: Daiichi Sankyo Inc, Basking Ridge, NJ, USA. [24]Present address: Eli Lilly, Indianapolis, IN, USA. [25]Present address: Gilead Sciences, Foster City, CA, USA. [26]These authors contributed equally: Kohei Shitara, Yelena Y. Janjigian. ✉e-mail: janjigiy@mskcc.org; ming.lei1@bms.com

Methods

Inclusion and ethics

This study was conducted in accordance with the trial protocol and with Good Clinical Practice guidelines developed by the International Council for Harmonisation. Written informed consent was obtained from all patients per the Declaration of Helsinki principles. The study is registered at ClinicalTrials.gov (NCT02872116).

Study design and patients

Key eligibility criteria and other study details of the CheckMate 649 study have been previously published[5,7]. Briefly, adult patients with previously untreated, unresectable or advanced gastric, gastroesophageal and esophageal adenocarcinoma were randomized to receive nivolumab-plus-chemotherapy, nivolumab-plus-ipilimumab or chemotherapy alone. Patients in the CheckMate 649 study who provided appropriate consent for the biomarker testing with evaluable baseline tumor tissue and matched whole-blood samples that passed the quality control (QC) criteria were eligible for the WES analyses, and those with evaluable baseline tumor samples that passed the QC criteria were eligible for the RNA-seq analyses. OS was assessed in patients with PD-L1 CPS ≥ 5 treated with nivolumab-plus-chemotherapy versus chemotherapy (primary end point), in all-randomized patients treated with nivolumab-plus-chemotherapy versus chemotherapy (secondary end point) and in patients with PD-L1 CPS ≥ 5 and all-randomized patients treated with nivolumab-plus-ipilimumab versus chemotherapy (secondary end point). Further details can be found in the supplementary information.

Definitions for gene alterations

Genes analyzed were selected based on previous mutational analyses in gastric or esophageal carcinoma[17,72]. For each gene of interest, an anticipated functional impact of alteration (gain of function or loss of function) was assigned based on previous evidence in gastric or esophageal carcinoma and/or other indications. Somatic mutations and copy number changes were mapped to each gene based on anticipated functional impact.

For mutations in genes with anticipated loss of function, individual somatic mutations were classified as loss of function if predicted to alter the amino acid sequence of a gene (specifically, frameshift mutations, mutations resulting in premature truncation and splice acceptor or donor variants) or if occurring at a known cancer hotspot[72]; deletions were classified as a loss of function alteration.

For mutations in genes with anticipated gain of function and recurrently mutated in cancer (and present in the list of hotspot mutations[73]), individual somatic mutations were classified as gain of function if occurring at a known recurrent hotspot. For mutations in genes with anticipated gain of function that were not recurrently mutated in cancer (not present in the list of hotspot mutations), any missense mutation was considered a gain of function; amplifications were classified as a gain-of-function alteration.

Oncoprint-style visualizations were generated using R package ComplexHeatmap (v.2.12.1); lollipop-style visualizations representing the location of mutations in *KRAS* were generated using the R package maftools (v.2.12).

Whole-exome sequencing

Baseline tumor tissue and matched whole-blood samples were processed using the Agilent SureSelect Human All Exon V6 in-solution hybrid capture panel and underwent subsequent next-generation sequencing on the Illumina NovaSeq platform. Sequence alignment and variant calling were performed. Specifically, BAM files were generated from the paired FASTQ files following the Broad Institute's best practices, using Sentieon implementation of the GATK pipeline[74,75]. The paired reads were aligned to the reference genome using the Burrows–Wheeler Aligner's Maximal Exact Match (BWA-MEM) algorithm[76–78] and sorted; duplicate reads were marked using Sentieon Dedup algorithm. During this process, Sentieon and Picard metrics were generated. A WES QC report was generated, which marked tumor samples PASS if total reads 45 million, mean target coverage 50× and depth of coverage >20× at 80% of the targeted capture region or higher. Normal samples were marked PASS if total reads 25 million, mean target coverage 25× and depth of coverage >20× at 80% of the targeted capture region or higher[79]. Somatic single-nucleotide variants and indels were then called by two variant callers: Tnscope (Sentieon Inc., based on and mathematically identical to the Broad Institute's MuTect2 (ref. 80) and Strelka2 (ref. 81)). A consensus set of PASS variants called by both Tnscope and Strelka2 for the targets and bait bed files of a WES capture kit was produced to capture high-confidence variants. Annotations were then added using SnpEff[82] from dbSNP[83], ExAC[84] and genomAD[85]. Variants either not present in or present at <0.01% allele frequency in the ExAC database[84] were retained for further analysis.

PD-L1 expression

PD-L1 expression was assessed at baseline in fresh biopsy specimens or from archival tumor tissue as described previously[5,7]. PD-L1 CPS was determined using a validated immunohistochemistry assay (Dako PD-L1 IHC 28-8 pharmDx assay; Agilent Technologies Inc.) as described previously[29].

TMB assessment

TMB was evaluated in patients who had sufficient WES to pass QC. Any variants that were found in gnomAD were excluded from the TMB calculation. Tissue TMB was defined as the total number of somatic missense mutations at the target region of capture kit used for the WES assay and identified by both Strelka2 and Tnscope somatic variant callers after filtering for the PASS variant only[86]. High TMB was defined as ≥199 mutations per exome and low TMB as <199 mutations per exome. The threshold of 199 mutations/exome is equivalent to ten mutations per megabase per Foundation Medicine F1CDx panel[87].

Detection of EBV in WES

PathSeq, a component of the Genome Analysis Toolkit (GATK)[88], was used to identify EBV reads from WES data. Specifically, reference genomes from both the host (human, hg38) and microbe (RefSeq bacteria and viral genomic sequences downloaded from ftp.ncbi.nlm.nih.gov/genomes/refseq/) were first prepared including index images construction, host k-mer library file generation and assembly of a taxonomy file derived from the microbe sequences, NCBI taxonomy dump (taxdump.tar.gz) and RefSeq accession catalog (RefSeq-release218.catalog.gz). PathSeq was then executed using the parameter '–is-host-aligned false' with a 90% sequence identity threshold set for the classification of microbial reads. Subsequently, the counts of reads mapped to EBV (taxonomy ID 10376) were extracted.

Genomic subtype classification

WES-evaluable tumor samples were categorized into four subtypes: EBV positive, hypermutated, GS and CIN. EBV-positive tumors were defined as those tumors with at least one read mapped to the EBV genome. For tumors without reads mapped to the EBV genome, a Gaussian mixture model was fitted to two metrics derived from WES data: TMB ($\log_{10}$ scale) and CIN score ($\log_{10}$ scale) using mclust (v.5.4.7) with no prior and default control parameters for expectation–maximization[89]. To quantify the degree of aneuploidy, GISTIC2.0 (ref. 90) was applied to the copy-number variation (CNV) data from the preprocessed WES data using GATK v.4.0. The CIN score was defined as the summation of square of gene-level GISTIC2.0 values as described previously[91]. The Bayesian information criterion was used to select the number of clusters ($n = 3$) that corresponds to hypermutated, GS and CIN subtypes and covariance parameterization. Tumors were assigned to clusters based on maximum probability of cluster membership.

Assessment of genomic alterations

MSI testing was conducted by Idylla MSI test of baseline tumor tissues. BROAD Best Practices Somatic CNV Panel Workflow (GATK v.4.1.0.0) and Control-FREEC LOH (v.11.6)[92] were run in parallel for CNV detection. High-confidence CNV calls from both tools were retained for further analysis. Amplifications were defined as a copy number of >3 and deletions were defined as a copy number <1.5 by both tools.

Gene expression profiling

Gene expression profiling was performed retrospectively using RNA-seq on a subset of baseline tumor samples. Pretreatment tumor tissues were processed using the Illumina TruSeq RNA Access in-solution hybrid capture panel and underwent subsequent next-generation sequencing on the Illumina NovaSeq platform. Paired-end FASTQ files were processed on Seven Bridges platform (Seven Bridges Genomics). Specifically, RNA-seq data were filtered by pre-aligning with STAR[93] to a microbial contaminant database downloaded from the National Center for Biotechnology Information GenBank. Samples with ≤5% of total reads mapping to the contamination database were aligned to the human genome (GRCh38) using the Ensembl 91 gene model and quantified using RSEM to optimally assign multimapping reads. Samples with <85% alignment rate were excluded from analysis. Sequencing quality was assessed using the Picard QC toolkit and DupRadar[94] to additionally quantify PCR artifacts using the following criteria: (1) Picard MarkDuplicates Estimated Library Size ≥3,000,000; (2) DupRadar Deduplicated Dynamic Range >265; (3) reads mapping to hemoglobin ≤5%; and (4) reads mapping to ribosomal regions ≤5%. Samples that failed to meet any of these criteria were excluded from the analysis.

Quantified raw counts from the remaining samples were normalized using edgeR trimmed mean of M (TMM) method[95] and normalized counts per million were $\log_2$ transformed for further analysis. TMM-normalized counts per million were *z*-scored (normalized to a mean of 0 and s.d. of 1) across all patients in the GES-evaluable group. For each patient, the GES score is defined as the median over the selected genes of the *z*-scored normalized expression values. The GES were categorized into tertiles (GES high, medium or low) by signature scores. The GES analyzed in all RNA-seq-evaluable patients are listed in Supplementary Table 4. For GES evaluations, moderate-to-strong correlations were defined as a Spearman's correlation of $\rho \geq 0.4$. The interaction between treatment and each GES score was assessed using LRT by comparing two models (model 1, OS ~ Arm + GES; model 2, OS ~ Arm + GES + Arm:GES), where Arm:GES refers to arm-by-GES interaction and GES was treated as a continuous value using a linear Cox proportional hazards (PH) model. Selected signatures (*P* from LRT <0.1) were used for further investigation by stratifying patients into tertiles based on signature scores.

GSEA methods

GSEA was performed to identify pathways and processes that may be associated with OS in three treatment arms as well as differential treatment effect in nivolumab-plus-chemotherapy or nivolumab-plus-ipilimumab versus chemotherapy. The association of expression of each gene with OS was evaluated using a Cox PH model (OS ~ Arm + Gene + Arm:Gene + Covariates) where Arm:Gene refers to arm-by-gene interaction. Gene refers to the continuous expression ($\log_2$ scale) of protein coding, constant regions of Ig (IG_C_gene) and T cell receptors (TR_C_gene). Covariates included prognostic factors such as age, sex, Eastern Cooperative Oncology Group performance status, region, primary tumor location, disease status, Lauren classification, peritoneal metastases, previous surgery related to current cancer or radiotherapy before randomization, number of organs with baseline lesion, signet ring cell and planned chemotherapy regimen as well as PD-L1 CPS level and RNA-seq batch ID. Reverse signed Wald test *z*-scores from the Cox PH models were ranked and then evaluated with the GSEA algorithm (fgsea v.1.16.0) on the HALLMARK gene sets from the Molecular Signatures Database[33,96] per arm and arm-by-gene interaction.

Statistical methods

All analyses were conducted using R v.4.0.3. Patient characteristics and clinical outcomes were compared between the biomarker-evaluable population and the intent-to-treat population using frequency statistics and descriptive statistics. Calculated *P* values were nominal (not adjusted for multiple testing unless otherwise stated), descriptive and not intended to demonstrate statistical significance. Survival analyses were conducted using the R survival (v.3.2-7) and survminer (https://github.com/kassambara/survminer) (v.0.4.8) packages. HR and 95% CIs for OS were assessed by unstratified Cox PH models and visualized using Kaplan–Meier analyses and forest plots. Comparisons among groups used Mann–Whitney *U*-test (two groups) and Kruskal–Wallis test (three or more groups) for continuous variables and chi-squared test for categorical variables.

Association of gene alterations with OS within subgroups of patients were tested using an unstratified Cox PH model. In tumors with higher TMB, higher likelihoods of gene mutations are expected; therefore, analysis of gene alteration status with outcomes control for TMB and MSI. Median OS and 95% CI were computed using a log–log-transformed model.

Reporting summary

Further information on research design is available in the Nature Portfolio Reporting Summary linked to this article.

Data availability

WES and RNA-seq datasets have been deposited in the European Genome–phenome Archive under study ID EGAS50000000747. Bristol Myers Squibb will honor legitimate requests for our clinical trial data from qualified researchers with a clearly defined scientific objective. Consistent with expectations of good scientific practice, researchers can request access to data from our studies by providing a research proposal with a commitment to publish their findings. The research proposal is reviewed by an independent review panel. We share data from Phase 2-4 interventional clinical trials completed on or after 1 January 2008 and evaluate medicines and indications approved in the US, EU and other designated markets. Data shared may include nonidentifiable patient-level and study-level clinical trial data, full clinical study reports and protocols. Sharing is subject to protection of patient privacy and respect for the patient's informed consent, and publication of the primary results in peer-reviewed journals. Bristol Myers Squibb reserves the right to update and change criteria at any time. Other criteria may apply, for details please visit Bristol Myers Squibb at www.vivli.org.

References

72. Cancer Genome Atlas Research Network. Integrated genomic characterization of oesophageal carcinoma. *Nature* **541**, 169–175 (2017).
73. Chang, M. T. et al. Accelerating discovery of functional mutant alleles in cancer. *Cancer Discov.* **8**, 174–183 (2018).
74. Weber, J. A., Aldana, R., Gallagher, B. D. & Edwards, J. S. Sentieon DNA pipeline for variant detection - software-only solution, over 20× faster than GATK 3.3 with identical results. *PeerJ Preprints* **4**, e1672v1672 (2016).
75. McKenna, A. et al. The Genome Analysis Toolkit: a MapReduce framework for analyzing next-generation DNA sequencing data. *Genome Res.* **20**, 1297–1303 (2010).
76. Li, H. Aligning sequence reads, clone sequences and assembly contigs with BWA-MEM. Preprint at https://arxiv.org/abs/1303.3997 (2013).

77. Li, H. & Durbin, R. Fast and accurate long-read alignment with Burrows–Wheeler transform. *Bioinformatics* **26**, 589–595 (2010).
78. Liu, Y. & Schmidt, B. Long read alignment based on maximal exact match seeds. *Bioinformatics* **28**, i318–i324 (2012).
79. Hellmann, M. D. et al. Tumor mutational burden and efficacy of nivolumab monotherapy and in combination with ipilimumab in small-cell lung cancer. *Cancer Cell* **33**, 853–861.e854 (2018).
80. Cibulskis, K. et al. Sensitive detection of somatic point mutations in impure and heterogeneous cancer samples. *Nat. Biotechnol.* **31**, 213–219 (2013).
81. Kim, S. et al. Strelka2: fast and accurate calling of germline and somatic variants. *Nat. Methods* **15**, 591–594 (2018).
82. Zook, J. M. et al. Integrating human sequence data sets provides a resource of benchmark SNP and indel genotype calls. *Nat. Biotechnol.* **32**, 246–251 (2014).
83. Sherry, S. T. dbSNP: the NCBI database of genetic variation. *Nucleic Acids Res.* **29**, 308–311 (2001).
84. Lek, M. et al. Analysis of protein-coding genetic variation in 60,706 humans. *Nature* **536**, 285–291 (2016).
85. Karczewski, K. J. et al. The mutational constraint spectrum quantified from variation in 141,456 humans. *Nature* **581**, 434–443 (2020).
86. Clark, M. J. et al. Performance comparison of exome DNA sequencing technologies. *Nat. Biotechnol.* **29**, 908–914 (2011).
87. Chang, H. et al. Bioinformatic methods and bridging of assay results for reliable tumor mutational burden assessment in non-small-cell lung cancer. *Mol. Diagn. Ther.* **23**, 507–520 (2019).
88. Kostic, A. D. et al. PathSeq: software to identify or discover microbes by deep sequencing of human tissue. *Nat. Biotechnol.* **29**, 393–396 (2011).
89. Scrucca, L., Fop, M., Murphy, T. B. & Raftery, A. E. mclust 5: clustering, classification and density estimation using Gaussian finite mixture models. *R J* **8**, 289–317 (2016).
90. Mermel, C. H. et al. GISTIC2.0 facilitates sensitive and confident localization of the targets of focal somatic copy-number alteration in human cancers. *Genome Biol.* **12**, R41 (2011).
91. Ock, C. Y. et al. Genomic landscape associated with potential response to anti-CTLA-4 treatment in cancers. *Nat. Commun.* **8**, 1050 (2017).
92. Boeva, V. et al. Control-FREEC: a tool for assessing copy number and allelic content using next-generation sequencing data. *Bioinformatics* **28**, 423–425 (2012).
93. Dobin, A. et al. STAR: ultrafast universal RNA-seq aligner. *Bioinformatics* **29**, 15–21 (2013).
94. Sayols, S., Scherzinger, D. & Klein, H. dupRadar: a Bioconductor package for the assessment of PCR artifacts in RNA-seq data. *BMC Bioinform.* **17**, 428 (2016).
95. Robinson, M. D. & Oshlack, A. A scaling normalization method for differential expression analysis of RNA-seq data. *Genome Biol.* **11**, R25 (2010).
96. Liberzon, A. et al. The Molecular Signatures Database (MSigDB) hallmark gene set collection. *Cell Syst.* **1**, 417–425 (2015).

Acknowledgements

This study was supported by Bristol Myers Squibb and Ono Pharmaceutical Co. We thank the patients and their families who made this study possible, the investigators and the clinical study teams at Bristol Myers Squibb and Ono Pharmaceutical Co. and Dako (an Agilent Technologies company) for collaborative development of the PD-L1 IHC 28-8 pharmDx assay. From Bristol Myers Squibb, we thank Translational Medicine program manager R. Menon and team lead, R. Novosiadly, biomarkers operations lead S. (Meeta) Panda and M.-S. Chien for support with developing the EBV and CIN algorithms. Professional medical writing assistance was provided by C. Dresch and D. Ramalingam of Parexel, funded by Bristol Myers Squibb.

Author contributions

K.S., Y.Y.J., J.A., M.M., D.P., L.S., P.D., M. Li and M. Lei contributed to the conception and design of the study in collaboration with Bristol Myers Squibb. K.S., Y.Y.J., J.A., M.M., L.S., M.G., C.G., L.W., K.Y., T.S., A.B., T.L., M.S., P.Y., R.K., M.K., T.Z., K.F. and E.E. recruited and/or treated patients, and all authors contributed to clinical or biomarker data acquisition. J.Y., X.W., A.C., D.P. and M. Lei performed biomarker analyses and J.Y. and A.C. conducted statistical analyses. J.Y., X.W., A.C., D.P., M. Li and M. Lei verified the data. All authors interpreted the data. All authors had access to all the data in the study, participated in developing or reviewing the paper and provided final approval to submit the paper for publication.

Competing interests

K.S. reports receiving personal fees for consulting and advisory roles from Bristol Myers Squibb, Takeda, Ono Pharmaceutical, Novartis, Daiichi Sankyo, Amgen, Boehringer Ingelheim, Merck Pharmaceutical, Astellas, Guardant Health Japan, Janssen, AstraZeneca, Zymeworks Biopharmaceuticals, ALX Oncology, Bayer, GlaxoSmithKline K.K., HEALIOS K.K., Moderna and Arcus Biosciences; receiving honoraria from Bristol Myers Squibb, Ono Pharmaceutical, Janssen, Eli Lilly, Astellas, and AstraZeneca; and receiving research funding (all to institution) from Astellas, Ono Pharmaceutical, Daiichi Sankyo, Taiho Pharmaceutical, Chugai, Merck Pharmaceutical, Amgen, Eisai, PRA Health Sciences Syneos Health, AstraZeneca, PPD-SNBL K.K. and TORAY. Y.Y.J. reports receiving research funding from the National Cancer Institute of the National Institutes of Health (to Memorial Sloan Kettering Cancer Center), Bayer, Bristol Myers Squibb, Cycle for Survival, Department of Defense, Fred's Team, Genentech/Roche Lilly, Merck, National Cancer Institute and Rgenix; serving as a consultant or in an advisory role for Basilea Pharmaceutical, Bayer, Bristol Myers Squibb, Daiichi Sankyo, Imugene, AstraZeneca, Lilly, Merck, Merck Serono, Michael J Hennessy Associates, Paradigm Medical Communications, Seattle Genetics, Pfizer, Rgenix, Amerisource-Bergen, Arcus Biosciences, Geneos, GlaxoSmithKline, Imedex, Lynx Health, Peerview, Silverback Therapeutics and Zymeworks; receiving stock options from Rgenix; and nonfinancial relationships with Clinical Care Options, Axis Medical Education and Research to Practice. J.A. reports receiving research grants from Amgen, Astellas Pharma, Bristol Myers Squibb, Daiichi Sankyo, Delta-Fly Pharma, Gilead Sciences, Lilly/ImClone, Merck, Novartis, ProLynx, Roche/Genentech, Taiho Pharmaceutical, Takeda and Zymeworks; serving as a consultant or in an advisory role for American Cancer Society, BeiGene, Bristol Myers Squibb, Insys Therapeutics, Merck, Novartis, Astellas Pharma, Gilead Sciences, Amgen, Servier, Geneos, Arcus Biosciences and Vaccinogen; receiving royalties from or holding patents and other intellectual property with Amgen, Bristol Myers Squibb, Genentech, Lilly, MedImmune, Merck, Roche and Taiho Pharmaceutical; and receiving honoraria from Acrotech BioPharma, Aduro Biotech, Amgen, Oncotherics, Astellas Pharma, BeiGene, Boehringer Ingelheim, Bristol Myers Squibb, Daiichi Sankyo, DAVA Pharmaceuticals, AstraZeneca, Fresenius Kabi, Gilead Sciences, Grail, Lilly, Merck, Novartis, Servier and Zymeworks. M.M. reports receiving research grants from Amgen, Leap Therapeutics, Merck Serono, AstraZeneca and Merck Sharp & Dohme; serving as a consultant or in an advisory role for Amgen, Bayer, BeiGene, Bristol Myers Squibb, Lilly, Merck Serono, Merck Sharp & Dohme, Pfizer, Roche, Servier, AstraZeneca and Taiho Pharmaceutical; receiving travel and accommodation expenses from American Society of Clinical Oncology, Amgen, Bayer, European Society for Medical Oncology, BeiGene, German Cancer Society, Merck Serono, Merck Sharp & Dohme and Roche; and receiving honoraria from Amgen, AstraZeneca/MedImmune, Bristol Myers Squibb, Merck Serono, Merck Sharp & Dohme Oncology, Roche/Genentech, Pierre Fabre, Sanofi and Servier. J.Y. reports being an employee of and holding stock in Bristol Myers Squibb. X.W. has no

competing interests to disclose. A.C. reports being employee of Bristol Myers Squibb; and holding stocks from Merck and Bristol Myers Squibb. D.P. reports being a former employee of Bristol Myers Squibb. L.S. reports receiving support for the present paper from Astellas and Oxford PharmaGenesis; receiving grants from Beijing Xiantong Biomedical Technology, Qilu Pharmaceutical, ZaiLab Pharmaceutical (Shanghai), Beihai Kangcheng (Beijing) Medical Technology, Yaojie Ankang (Nanjing) Technology Co., Ltd, Baiji Shenzhou (Beijing) Biotechnology Co., Ltd and Jacobio Pharmaceuticals; receiving consulting fees from Mingji Biopharmaceutical, Haichuang Pharmaceutical and Herbour Biomed; receiving honoraria from Hutchison Whampoa, Hengrui, ZaiLab and CSTONE Pharmaceutical; and participation on advisory board for Merck Sharp & Dohme, Merck, Bristol Myers Squibb, Boehringer Ingelheim, Sanofi, Roche, Servier and AstraZeneca. M.G. reports receiving research grants from Bristol Myers Squibb and Novartis; receiving speakers' bureau fees from Bayer, Bristol Myers Squibb and Merck; receiving travel and accommodation expenses from Roche; and serving as a consultant or in an advisory role for Merck Sharp & Dohme, AstraZeneca and Roche. C.G. reports receiving research grants from Bristol Myers Squibb, AstraZeneca and Merck; receiving speakers' bureau fees from AstraZeneca, Merck and Bristol Myers Squibb; serving as a consultant or in an advisory role for Merck, Tecnofarma and AstraZeneca; and honoraria from AstraZeneca, Merck and Roche. L.W. reports receiving speakers' bureau fees from Bristol Myers Squibb; receiving travel and accommodation expenses from Servier; receiving honoraria from BeiGene, Bristol Myers Squibb and Merck Sharp & Dohme; and serving in a consulting or advisory role for GlaxoSmithKline and Servier. K.Y. reports receiving research grants from Boehringer Ingelheim, Bristol Myers Squibb, Chugai Pharma, Daiichi Sankyo, Eisai, Gilead Sciences, Lilly, Merck Sharp & Dohme Oncology, Ono Pharmaceutical, Sanofi, Taiho Pharmaceutical and Yakult Honsha; receiving speakers' bureau fees from Bristol Myers Squibb Japan, Chugai Pharma, Daiichi Sankyo, Lilly, Merck, Ono Pharmaceutical, Taiho Pharmaceutical and Takeda; and serving as a consultant or in an advisory role for Bristol Myers Squibb Japan and Daiichi Sankyo. T.S. reports receiving support for the present paper from Bristol Myers Squibb. A.B. reports receiving speakers' bureau fees from AstraZeneca, Bristol Myers Squibb/Medarex and Merck. T.L. has no competing interests to disclose. M.S. reports receiving research funding from AbbVie, Amgen, Astellas Pharma, AstraZeneca, BeiGene, Bioven, Clovis Oncology, Five Prime Therapeutics, Bristol Myers Squibb, Eli Lilly, Gilead Sciences, Merck Sharp & Dohme, Mylan, GlaxoSmithKline, Novartis, Pfizer/EMD Serono, Tesaro, Sanofi/Regeneron and Roche; and receiving travel accommodations and expenses from Bristol Myers Squibb. P.Y. has no competing interests to disclose. R.K. reports receiving research grants from Amgen, AstraZeneca, Bristol Myers Squibb, Eli Lilly, PPD, GlaxoSmithKline, Labcorp Drug Development, Gaico, Janssen Cliag Farmaceútica, Gilead Sciences, Parexel, Syneos Health, Novartis, Pfizer, Roche SAQ, Merck Sharp & Dohme and Sanofi; receiving support for the present paper from Bristol Myers Squibb, Merck Sharp & Dohme and Astellas Pharma; receiving consulting fees from Astellas Pharma, Bristol Myers Squibb, Merck Sharp & Dohme and Roche; honoraria or speakers bureaus from Astellas Pharma, Bristol Myers Squibb, Merck Sharp & Dohme, Raffo and Roche; receiving travel and accommodation expenses from Bristol Myers Squibb, Merck Sharp & Dohme, Raffo, Gador, Pfizer and Roche; and reports leadership or fiduciary role in other board, society, committee or advocacy group as Academic Director Argentine Association of Clinical Oncology. M.K. has no competing interests to disclose. T.Z. reports consulting or advisory roles for Bristol Myers Squibb, Merck Sharp & Dohme Oncology, Novartis, Pfizer and Roche. K.F. has no competing interests to disclose. E.E. reports being a consultant for Bristol Myers Squibb, Zymeworks, Adaptimmune, BeiGene, Jazz, Astellas, Virecta Tx, Signatera, AbbVie and Daiichi Sankyo; grant/research support from Bristol Myers Squibb, Bold Therapeutics, Zymeworks, AstraZeneca Canada, Amgen and Jazz; and having a family member work for Merck. P.D. reports being an employee of Bristol Myers Squibb at the time of study conduct. M. Li reports receiving support for the present paper, honoraria, holding stocks in, and being an employee of Bristol Myers Squibb. M. Lei reports pending patents with, holding stocks in, and being an employee of Bristol Myers Squibb.

Additional information

Extended data is available for this paper at https://doi.org/10.1038/s41591-025-03575-0.

Supplementary information The online version contains supplementary material available at https://doi.org/10.1038/s41591-025-03575-0.

Correspondence and requests for materials should be addressed to Yelena Y. Janjigian or Ming Lei.

Peer review information *Nature Medicine* thanks Sheng Luo, Ken Kato and the other, anonymous, reviewer(s) for their contribution to the peer review of this work. Primary Handling Editor: Ulrike Harjes, in collaboration with the *Nature Medicine* team.

https://doi.org/10.1038/s41591-025-03575-0

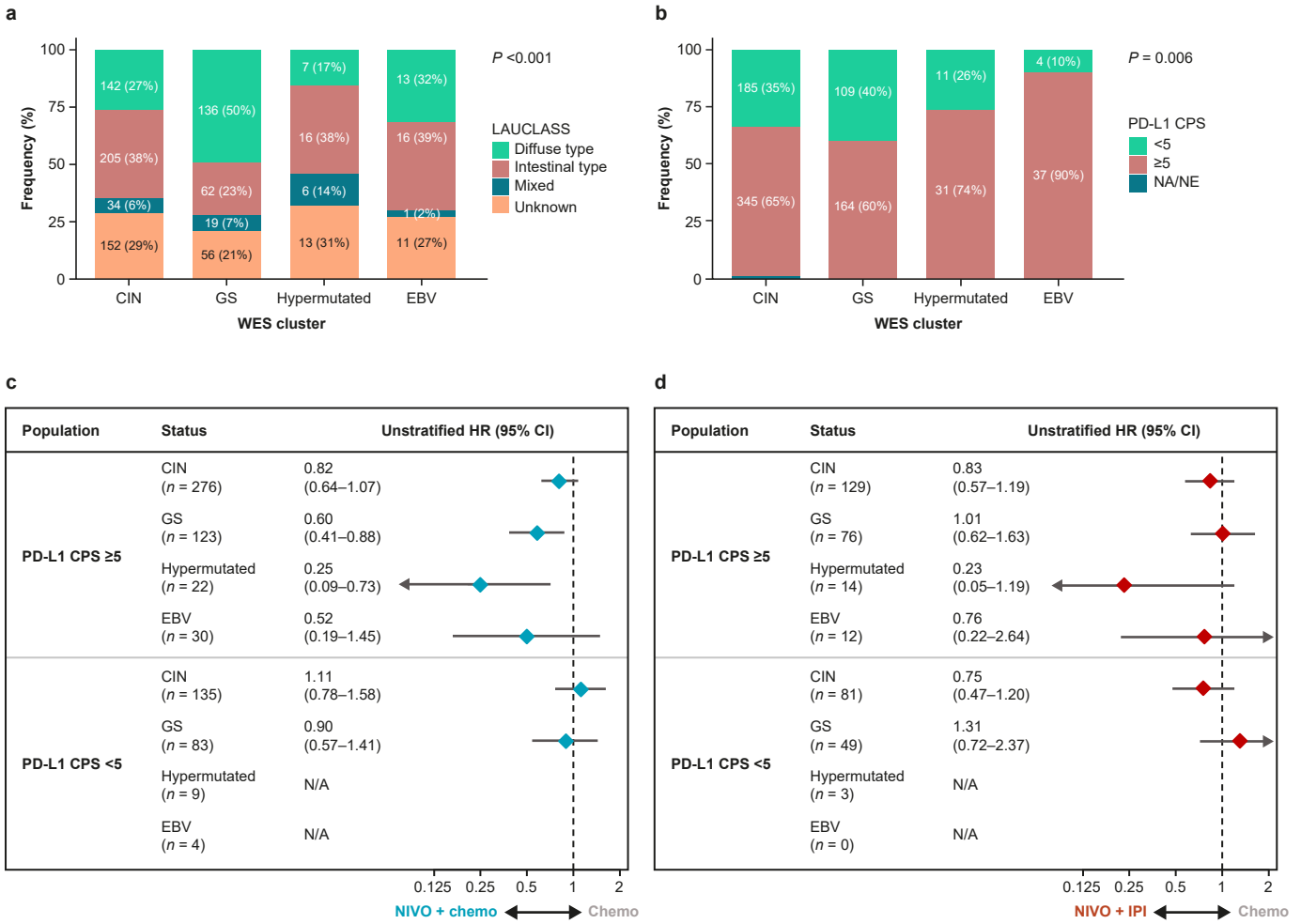

Extended Data Fig. 1 | Genomic characterization of baseline tumors from CheckMate 649. a and **b**, Tumor characterization subtyping by genomic subtypes and histology (**a**), or PD-L1 CPS (**b**). *P* values are based on two-sided Chi-squared test. Exact *P* value for (**a**) was 6.673e-09. **c** and **d**, Forest plot of OS by genomic subsets in all WES-evaluable patients treated with nivolumab-plus-chemotherapy (**c**) or nivolumab-plus-ipilimumab (**d**) versus chemotherapy. Data are presented as unstratified HRs and 95% CI. HR was not calculated if the number of patients in each arm was less than 5. CIN, chromosomal instability; CPS, combined positive score; EBV, Epstein–Barr virus; GS, genomically stable; IPI, ipilimumab; MSI-H, microsatellite instability high; MSS, microsatellite stable; N/A, not available; NIVO, nivolumab; PD-L1, programmed death ligand 1; TMB, tumor mutational burden; WES, whole-exome sequencing.

https://doi.org/10.1038/s41591-025-03575-0

a

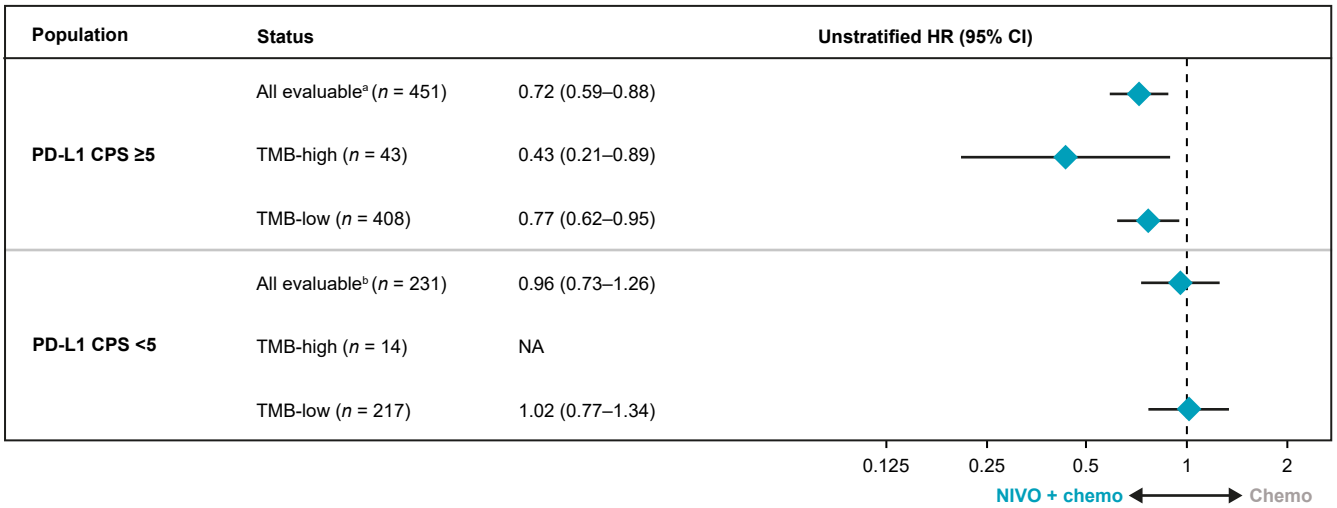

b

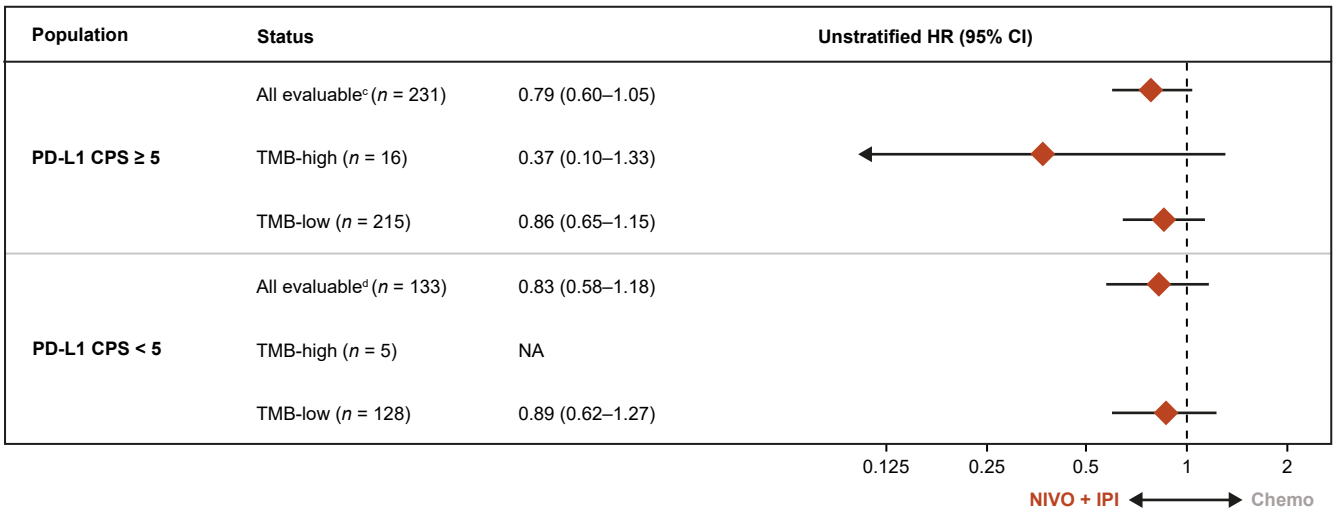

Extended Data Fig. 2 | OS by PD-L1 CPS and TMB status in patients treated with nivolumab-plus-chemotherapy or nivolumab-plus-ipilimumab versus chemotherapy. a, Forest plot showing OS by baseline PD-L1 CPS and TMB status in patients who received nivolumab-plus-chemotherapy versus chemotherapy. **b**, Forest plot showing OS by baseline PD-L1 CPS and TMB status in patients who received nivolumab-plus-ipilimumab versus chemotherapy. Data are presented as unstratified HRs and 95% CI. [a]TMB not evaluable/available in 504 patients (NIVO+chemo: $n = 238$; chemo: $n = 266$). [b]TMB not evaluable/available in 376 patients (NIVO+chemo: $n = 185$; chemo: $n = 191$). [c]TMB not evaluable/available in 243 patients (NIVO+IPI: $n = 121$; chemo: $n = 122$). [d]TMB not evaluable/available in 191 patients (NIVO+IPI: $n = 98$; chemo: $n = 93$). Chemo, chemotherapy; CI, confidence interval; CPS, combined positive score; HR, hazard ratio; NA, not available; NIVO, nivolumab; OS, overall survival; PD-L1, programmed death ligand 1; TMB, tumor mutational burden; WES, whole-exome sequencing.

https://doi.org/10.1038/s41591-025-03575-0

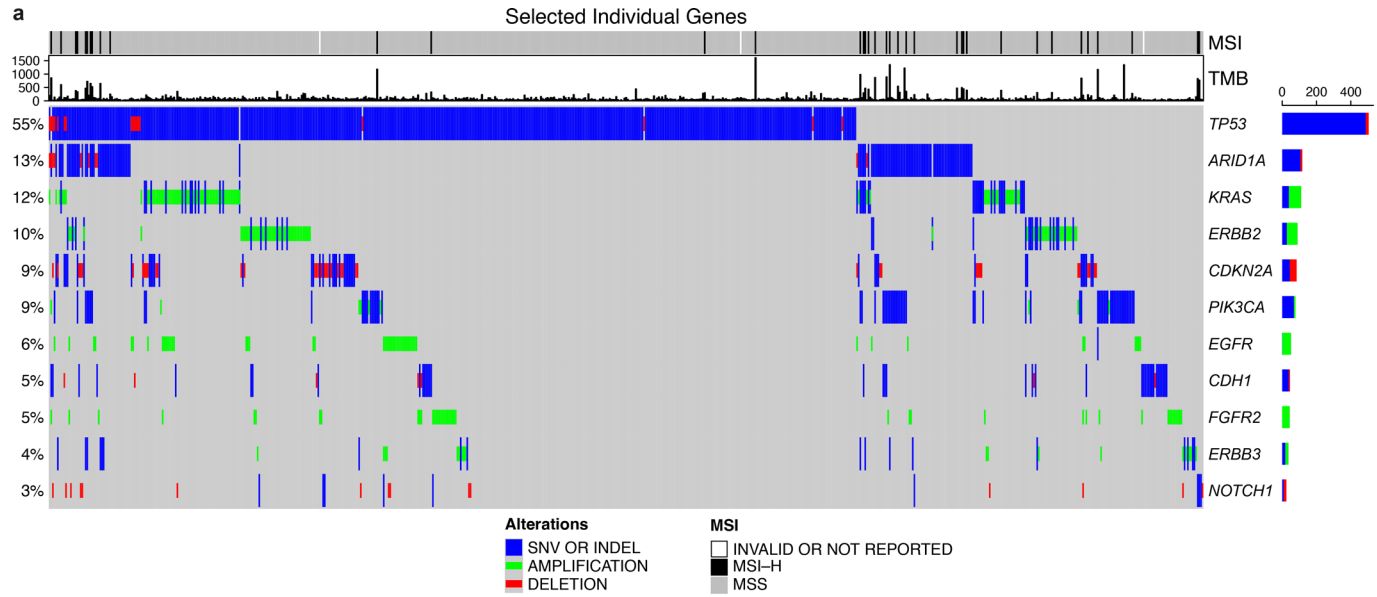

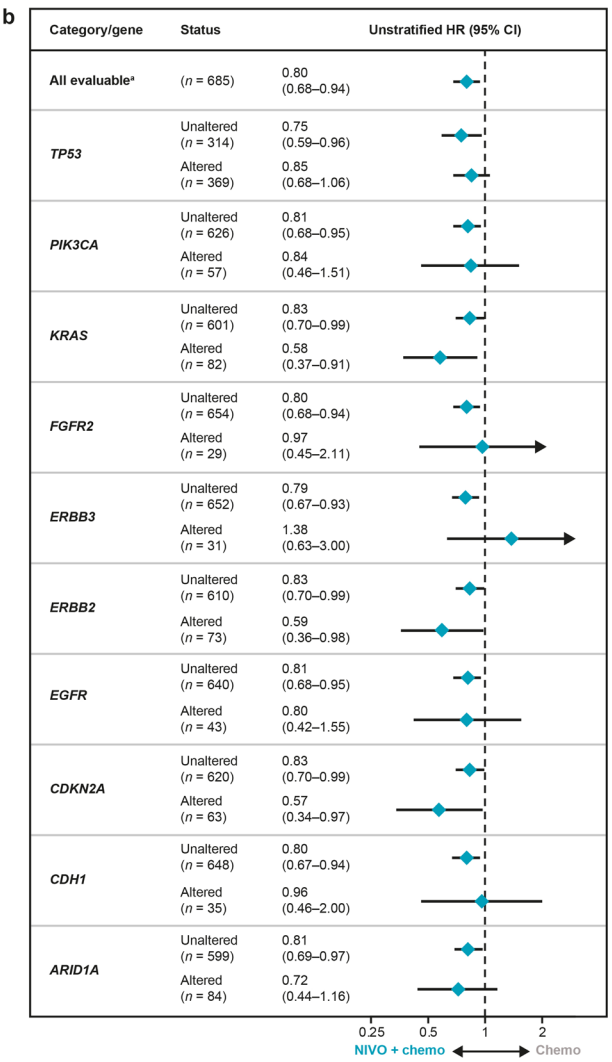

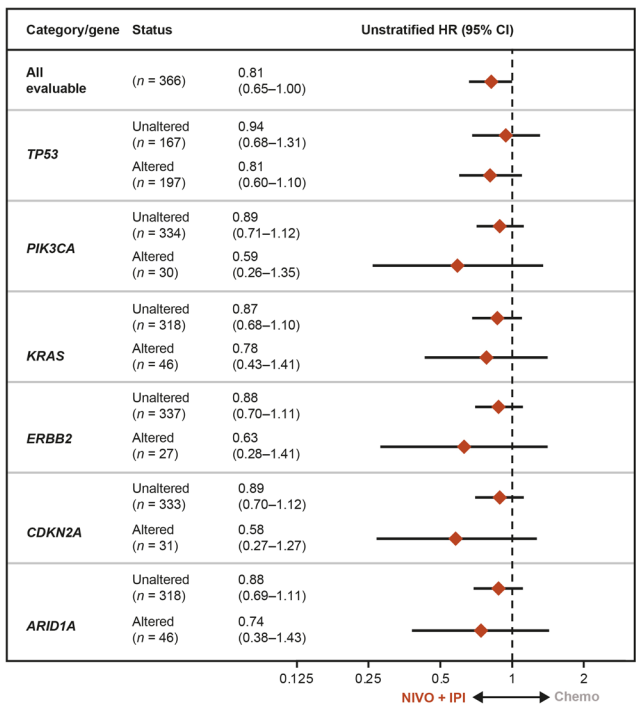

Extended Data Fig. 3 | OS by gene alterations. a, Oncoprints of gene alterations among all WES-evaluable patients. Frequency and overlap of select gene alterations. **b** and **c**, Forest plots showing the association between OS and selected gene alterations in patients who received nivolumab-plus-chemotherapy versus chemotherapy (**b**) or nivolumab-plus-ipilimumab versus chemotherapy (**c**). Data are presented as unstratified HRs and 95% CI. HR was not calculated if the number of patients in each arm was less than 10. HR were derived from model including interaction of gene alteration status with treatment, MSI and TMB status. [a]MSI status not evaluable/available in 2 patients. Chemo, chemotherapy; CI, confidence interval; CPS, combined positive score; HR, hazard ratio; IPI, ipilimumab; MSI-H, microsatellite instability high; N/A, not available; NIVO, nivolumab; OS, overall survival; WES, whole-exome sequencing.

https://doi.org/10.1038/s41591-025-03575-0

a

GES (LRT; *P* <0.1)	All evaluable	PD-L1 CPS ≥5	PD-L1 CPS <5
6-gene angiogenesis	0.033	0.046	0.214
16-gene angiogenesis	0.019	0.047	0.213
5-gene angiogenesis	0.057	0.042	0.360
7-gene angiogenesis	0.018	0.028	0.228
30-gene glycolysis	0.849	0.996	0.976
101-gene hypoxia	0.748	0.940	0.689
20-gene hypoxia	0.814	0.745	0.319
10-gene inflammatory	0.297	0.964	0.710
12-gene chemokine	0.345	0.958	0.671
2-gene regulatory T cell	0.717	0.323	0.578
5-gene MAPK	0.056	0.103	0.304
34-gene MAPK	0.299	0.727	0.322
14-gene MAPK	0.782	0.464	0.793
227-gene proliferation	0.242	0.639	0.270
12-gene EMT	0.283	0.133	0.920
9-geneTGFbeta	0.345	0.221	0.896
15-gene stroma	0.087	0.058	0.730

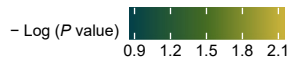

b

GES (LRT; *P* <0.1)	All evaluable	PD-L1 CPS ≥5	PD-L1 CPS <5
6-gene angiogenesis	0.349	0.110	0.678
16-gene angiogenesis	0.294	0.116	0.597
5-gene angiogenesis	0.135	0.035	0.741
7-gene angiogenesis	0.083	0.013	0.746
30-gene glycolysis	0.020	0.041	0.574
101-gene hypoxia	0.032	0.050	0.887
20-gene hypoxia	0.019	0.074	0.504
10-gene inflammatory	0.045	0.082	0.583
12-gene chemokine	0.035	0.079	0.601
2-gene regulatory T cell	0.026	0.082	0.310
5-gene MAPK	0.122	0.012	0.956
34-gene MAPK	0.055	0.057	0.759
14-gene MAPK	0.038	0.112	0.379
227-gene proliferation	0.070	0.017	0.928
12-gene EMT	0.813	0.888	0.756
9-geneTGFbeta	0.863	0.620	0.873
15-gene stroma	0.020	0.007	0.708

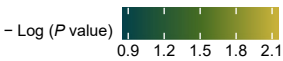

Extended Data Fig. 4 | Association test of differential OS treatment effect by GES scores in patients treated with nivolumab-plus-chemotherapy or with nivolumab-plus-ipilimumab versus chemotherapy. a, *P* value of interaction between GES score and treatment arm among all RNA-seq-evaluable patients and by PD-L1 CPS status who received nivolumab-plus-chemotherapy versus chemotherapy. Selected gene signatures with *P* values < 0.1 from Likelihood Ratio Test are colored in the table; color scale is shown at the bottom. **b**, *P* value of interaction between GES score and treatment arm among all RNA-seq-evaluable patients and by PD-L1 CPS status who received nivolumab-plus-ipilimumab versus chemotherapy. Selected gene signatures with *P* values < 0.1 from Likelihood Ratio Test are colored in the table; color scale is shown at the bottom. Selected gene signatures with *P* values < 0.1 from Likelihood Ratio Test are colored in the table; color scale is shown at the bottom.

https://doi.org/10.1038/s41591-025-03575-0

a

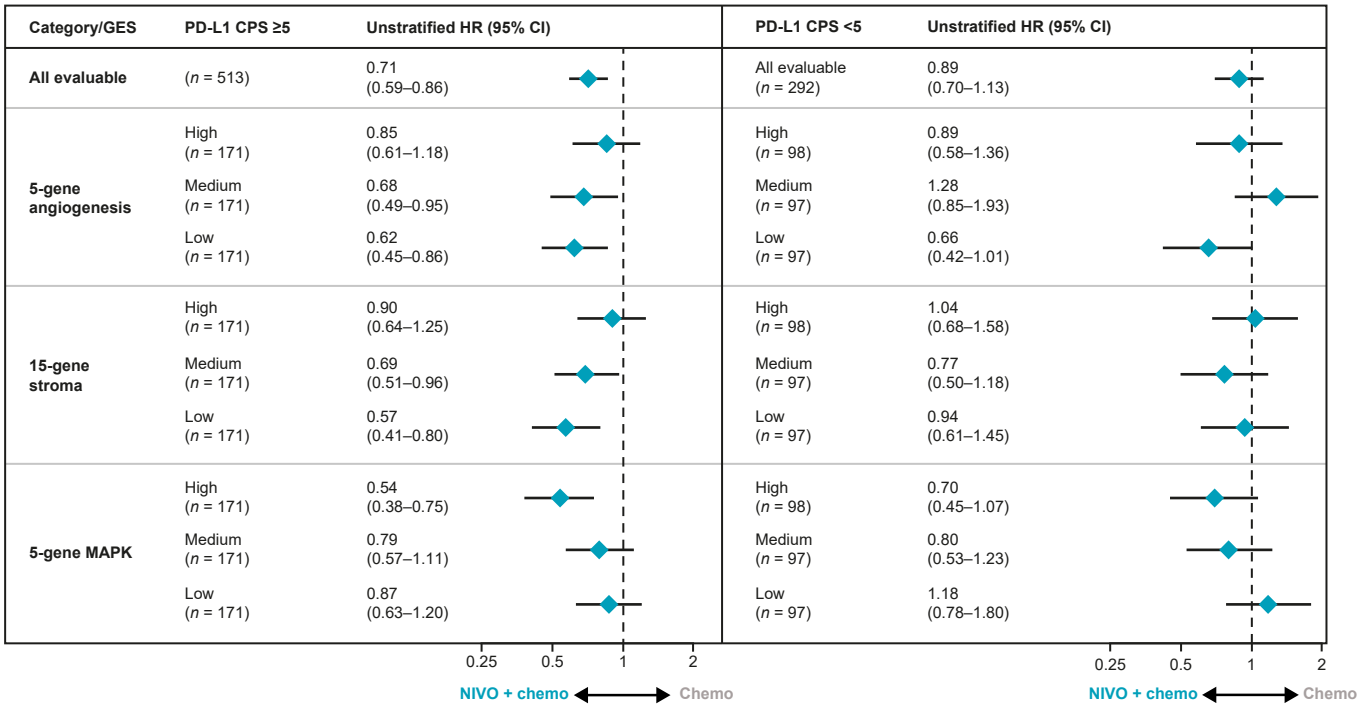

b

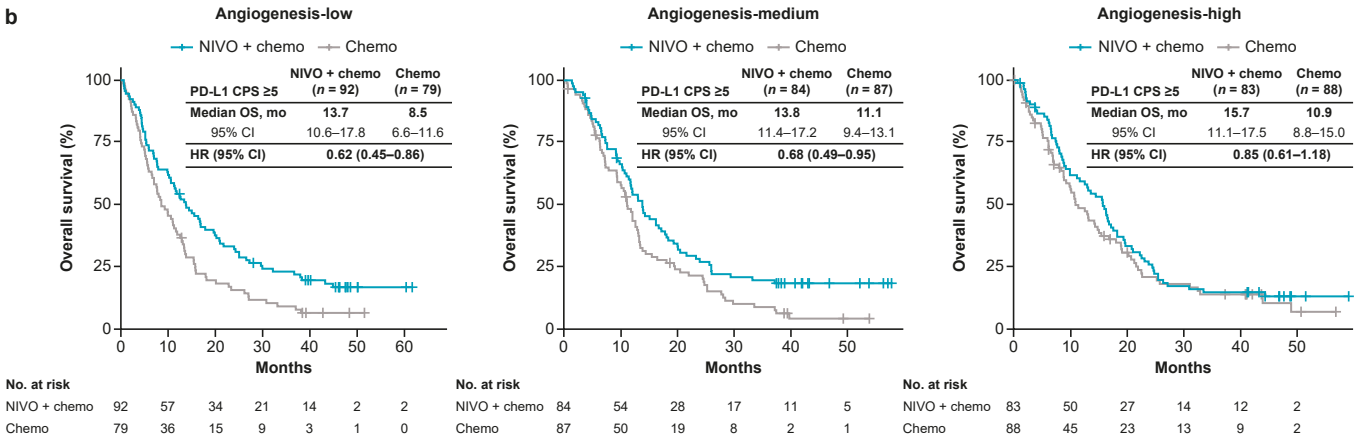

c

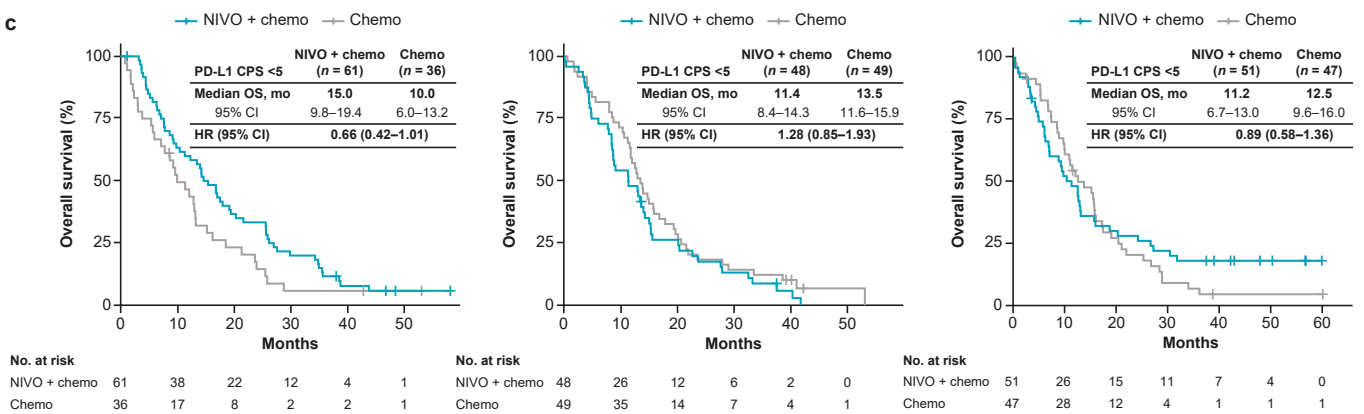

Extended Data Fig. 5 | OS by GES scores and PD-L1 CPS status in patients treated with nivolumab-plus-chemotherapy versus chemotherapy. **a**, Forest plot showing the correlation between OS and selected signatures used to stratify patients into tertiles (high, medium, or low). Data are presented as unstratified HRs and 95% CI. HR was not calculated if the number of patients in each arm was less than 5. **b** and **c**, Kaplan–Meier estimates of OS in all RNA-seq-evaluable patients with low, medium or high angiogenesis GES scores (5-gene angiogenesis) and PD-L1 CPS ≥ 5 (**b**) or PD-L1 CPS < 5 (**c**) at baseline. Chemo, chemotherapy; CI, confidence interval; CPS, combined positive score; GES, gene expression signature; HR, hazard ratio; NIVO, nivolumab; OS, overall survival; PD-L1, programmed death ligand 1.

https://doi.org/10.1038/s41591-025-03575-0

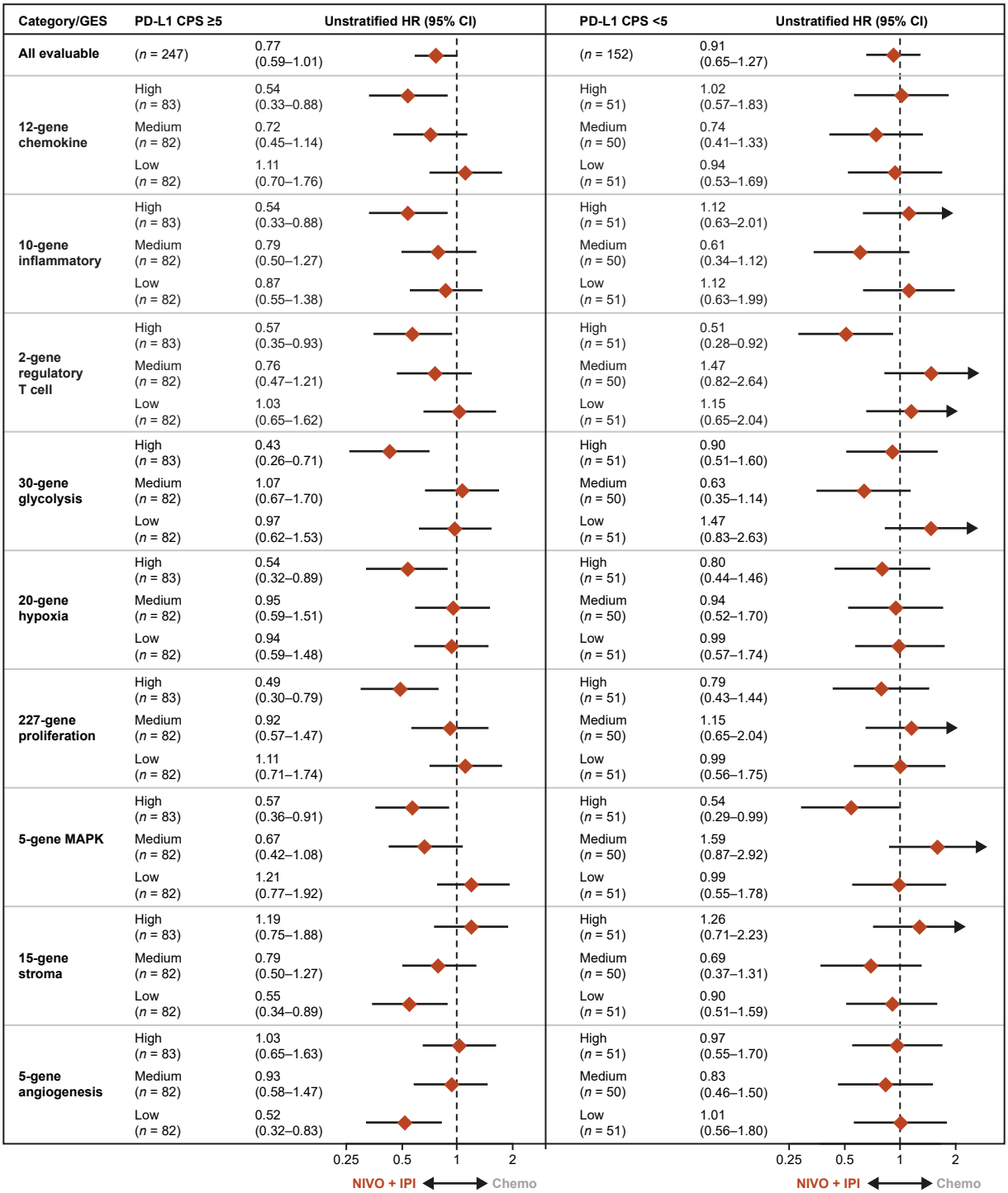

Extended Data Fig. 6 | OS by GES scores and PD-L1 CPS status in patients treated with nivolumab-plus-ipilimumab versus chemotherapy. Forest plot showing the correlation between OS and selected signatures used to stratify patients into tertiles (high, medium versus low). Data are presented as unstratified HRs and 95% CI. HR was not calculated if the number of patients in each arm was less than 5. CI, confidence interval; CPS, combined positive score; GES, gene expression signature; HR, hazard ratio; PD-L1, programmed death ligand 1.

https://doi.org/10.1038/s41591-025-03575-0

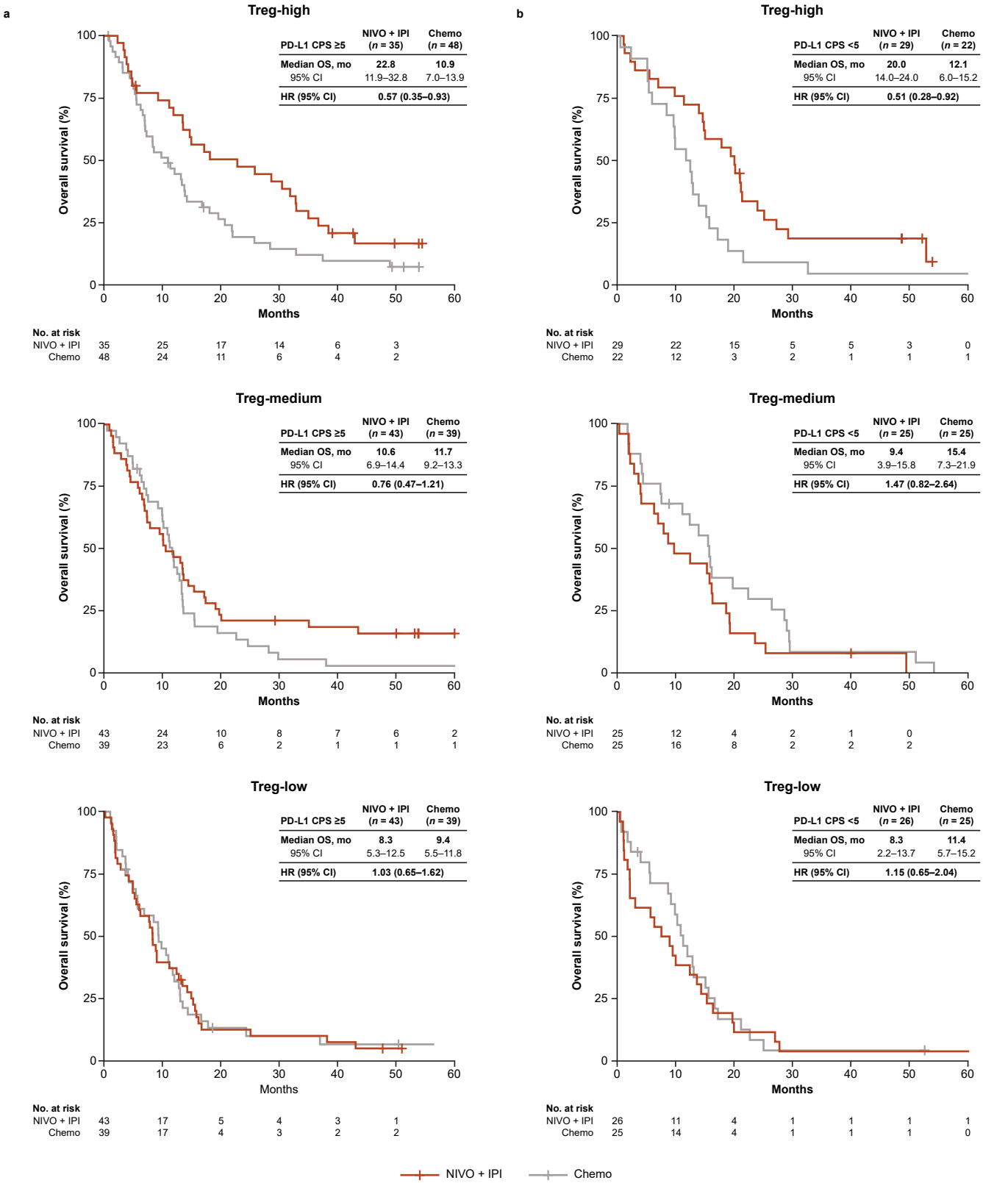

Extended Data Fig. 7 | OS by PD-L1 CPS and Treg status in patients treated with nivolumab-plus-ipilimumab versus chemotherapy. a and **b**, Kaplan–Meier estimates of OS in all RNA-seq-evaluable patients with high, medium or low regulatory T cell GES scores (2-gene regulatory T cell) and PD-L1 CPS ≥ 5 (**a**) or PD-L1 CPS < 5 (**b**) at baseline. Chemo, chemotherapy; CI, confidence interval; CPS, combined positive score; HR, hazard ratio; IPI, ipilimumab; NIVO, nivolumab; OS, overall survival; PD-L1, programmed death ligand 1.

https://doi.org/10.1038/s41591-025-03575-0

Comparison	Factors potentially associated with efficacy				Factors potentially associated with lack of efficacy			
		All	PD-L1 CPS ≥5	PD-L1 CPS <5		All	PD-L1 CPS ≥5	PD-L1 CPS <5
NIVO + chemo versus Chemo	TMB-high	Yes	Yes	Yes	Angiogenesis GES	Yes[a]	Yes[a]	Yes[a]
	MAPK GES	Yes[a]	Yes[a]	Yes	Stroma GES	Yes[a]	Yes[a]	No
NIVO + IPI versus Chemo	TMB-high	Yes	Yes	No	Stroma GES	Yes[a]	Yes[a]	No
	MAPK GES	Yes[a]	Yes[a]	Yes				
	Inflammatory GES	Yes[a]	Yes[a]	No				
	Treg GES	Yes[a]	Yes[a]	Yes	Angiogenesis GES	Yes[a]	Yes[a]	No
	Proliferation GES	Yes[a]	Yes[a]	No				
	Glycolysis GES	Yes[a]	Yes[a]	No				
	Hypoxia GES	Yes[a]	Yes[a]	No				

Extended Data Fig. 8 | Correlations between biomarkers in patients treated with nivolumab-plus-chemotherapy, nivolumab-plus-ipilimumab or chemotherapy. Summary of factors potentially associated with efficacy with nivolumab-plus-chemotherapy or nivolumab-plus-ipilimumab. [a]Indicates significant association with treatment when treated as a continuous variable ($P < 0.1$). These exploratory P values are not meant to show statistical significance and are intended to describe the relative performance of the different signatures for association with response. Chemo, chemotherapy; CPS, combined positive score; GES, gene expression signatures; IPI, ipilimumab; NIVO, nivolumab; PD-L1, programmed death ligand 1; TMB, tumor mutational burden.

https://doi.org/10.1038/s41591-025-03575-0

	NIVO + chemo versus Chemo			NIVO + IPI versus Chemo		
Interferon_gamma_response	2.87 (5e–10)	2.55 (2e–09)	1.49 (0.007)	3.08 (5e–10)	1.76 (3e–04)	2.63 (8e–10)
Oxidative_phosphorylation	1.55 (0.002)	1.57 (0.007)	0.63 (1.000)	2.75 (5e–10)	1.66 (0.001)	2.14 (8e–09)
Interferon_alpha_response	2.57 (5e–10)	2.28 (6e–08)	1.35 (0.105)	2.93 (5e–10)	2.20 (9e–07)	2.37 (1e–08)
Unfolded_protein_response	1.97 (2e–05)	1.05 (0.500)	1.69 (0.002)	2.56 (5e–10)	1.35 (0.116)	1.95 (6e–05)
MYC_targets_v2	2.75 (5e–10)	–1.34 (0.176)	2.77 (1e–09)	2.96 (5e–10)	0.64 (0.996)	2.91 (8e–10)
Mtorc1_signaling	2.20 (5e–10)	–1.13 (0.349)	2.47 (1e–09)	3.16 (5e–10)	1.21 (0.228)	3.01 (8e–10)
G2m_checkpoint	3.22 (5e–10)	–1.16 (0.268)	3.15 (1e–09)	3.36 (5e–10)	0.70 (0.996)	3.37 (8e–10)
E2f_targets	3.57 (5e–10)	–1.12 (0.371)	3.39 (1e–09)	3.66 (5e–10)	0.77 (0.996)	3.60 (8e–10)
DNA_repair	2.09 (2e–07)	1.08 (0.486)	1.77 (7e–04)	2.67 (5e–10)	1.42 (0.068)	2.32 (2e–09)
Allograft_rejection	2.61 (5e–10)	2.26 (2e–09)	1.47 (0.012)	2.55 (5e–10)	1.43 (0.043)	2.24 (9e–10)
MYC_targets_v1	3.14 (5e–10)	–1.81 (3e–05)	3.40 (1e–09)	3.57 (5e–10)	–1.15 (0.231)	3.75 (8e–10)
Spermatogenesis	1.89 (3e–05)	–0.68 (1.000)	1.76 (0.001)	1.62 (0.004)	–0.77 (0.996)	1.35 (0.060)
IL6_JAK_STAT3_signaling	1.43 (0.059)	1.98 (6e–05)	–1.06 (0.599)	2.09 (6e–06)	1.17 (0.323)	1.86 (4e–04)
Mitotic_spindle	1.30 (0.093)	–1.68 (5e–04)	1.70 (4e–04)	1.94 (1e–06)	–1.63 (0.001)	2.17 (3e–09)
UV_response_up	1.05 (0.425)	0.90 (0.831)	1.00 (0.709)	2.00 (8e–07)	1.22 (0.231)	1.80 (1e–04)
Tnfa_signaling_via_nfkb	–1.39 (0.019)	–1.49 (0.012)	–0.79 (1.000)	1.96 (7e–07)	–1.19 (0.231)	1.93 (2e–06)
Pi3k_akt_mtor_signaling	1.41 (0.065)	0.92 (0.780)	1.21 (0.302)	2.01 (2e–05)	1.12 (0.350)	2.10 (3e–06)
P53_pathway	–1.07 (0.363)	1.07 (0.486)	–1.48 (0.012)	1.77 (6e–05)	0.89 (0.931)	1.56 (0.002)
Inflammatory_response	1.08 (0.376)	1.38 (0.046)	–0.78 (1.000)	1.73 (1e–04)	0.85 (0.980)	1.70 (2e–04)
IL2_STAT5_signaling	1.32 (0.085)	1.10 (0.456)	1.04 (0.599)	1.54 (0.002)	–0.76 (0.996)	1.60 (0.001)
Glycolysis	–1.18 (0.153)	–1.39 (0.042)	0.93 (0.921)	1.97 (5e–07)	1.12 (0.350)	1.60 (0.001)
Fatty_acid_metabolism	0.72 (0.989)	1.03 (0.547)	–0.96 (0.843)	1.48 (0.008)	1.58 (0.008)	0.82 (0.940)
Apoptosis	0.97 (0.579)	1.08 (0.486)	–0.77 (1.000)	1.59 (0.003)	0.80 (0.996)	1.64 (8e–04)
Reactive_oxygen_species_pathway	0.73 (0.939)	1.19 (0.432)	–0.88 (0.921)	2.06 (3e–05)	1.65 (0.046)	1.36 (0.113)
Complement	1.10 (0.339)	1.07 (0.486)	0.59 (1.000)	1.48 (0.008)	1.19 (0.231)	1.10 (0.306)
Cholesterol_homeostasis	0.65 (0.989)	–0.85 (0.921)	0.78 (1.000)	1.65 (0.006)	1.44 (0.112)	0.99 (0.581)
Adipogenesis	–1.28 (0.065)	0.78 (1.000)	–1.13 (0.347)	1.44 (0.008)	1.33 (0.092)	0.99 (0.600)
Pancreas_beta_cells	0.56 (0.989)	1.14 (0.456)	–0.89 (0.921)	–1.58 (0.016)	1.48 (0.115)	–1.93 (8e–04)
Estrogen_response_early	–1.74 (4e–05)	–0.99 (0.643)	–1.47 (0.012)	1.03 (0.439)	0.88 (0.931)	1.06 (0.379)
Apical_junction	–1.73 (5e–05)	–1.42 (0.036)	–1.15 (0.334)	–0.89 (0.881)	–1.43 (0.035)	0.99 (0.581)
Hypoxia	–2.17 (3e–09)	–1.89 (2e–05)	–1.06 (0.565)	1.14 (0.218)	–1.20 (0.230)	1.19 (0.152)
Coagulation	–1.82 (9e–05)	–1.45 (0.047)	–1.06 (0.599)	–1.61 (0.003)	–1.08 (0.350)	–1.24 (0.130)
TGF_beta_signaling	–1.94 (5e–04)	–1.79 (0.007)	–1.10 (0.561)	0.64 (0.997)	–2.05 (5e–04)	1.42 (0.058)
KRAS_signaling_dn	–1.24 (0.081)	1.28 (0.122)	–1.63 (0.001)	–1.75 (1e–04)	1.12 (0.350)	–1.72 (1e–04)
UV_response_dn	–2.02 (7e–07)	–2.21 (2e–07)	–0.80 (1.000)	–1.97 (4e–06)	–2.09 (9e–06)	–1.16 (0.238)
Myogenesis	–2.38 (5e–10)	–1.48 (0.008)	–1.50 (0.006)	–1.86 (5e–06)	–1.45 (0.029)	–1.40 (0.024)
Epithelial_mesenchymal_transition	–2.75 (5e–10)	–2.75 (2e–09)	–0.68 (1.000)	–1.55 (0.002)	–2.45 (5e–09)	0.86 (0.927)
	NIVO + chemo	Chemo	Interaction	NIVO + IPI	Chemo	Interaction

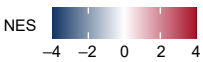

Extended Data Fig. 9 | Gene set enrichment analysis in patients treated with nivolumab-plus-chemotherapy or nivolumab-plus-ipilimumab versus chemotherapy. Enrichment of genes associated with OS in nivolumab-plus-chemotherapy, nivolumab-plus-ipilimumab, or chemotherapy as well as the genes with differential OS association by treatment arm (interaction) using chemotherapy as the reference. The data are shown as NES (adjusted *P* value) and the cells are colored if adjusted *P* value is < 0.01. The strength of association is shown as a color scale at the bottom. Chemo, chemotherapy; IPI, ipilimumab; NES, normalized enrichment score; NIVO, nivolumab; OS, overall survival.

nature portfolio

Corresponding author(s): Yelena Y Janjigian

Last updated by author(s): Jan 8, 2025

Reporting Summary

Nature Portfolio wishes to improve the reproducibility of the work that we publish. This form provides structure for consistency and transparency in reporting. For further information on Nature Portfolio policies, see our Editorial Policies and the Editorial Policy Checklist.

Statistics

For all statistical analyses, confirm that the following items are present in the figure legend, table legend, main text, or Methods section.

n/a	Confirmed
☐	☒ The exact sample size (*n*) for each experimental group/condition, given as a discrete number and unit of measurement
☒	☐ A statement on whether measurements were taken from distinct samples or whether the same sample was measured repeatedly
☐	☒ The statistical test(s) used AND whether they are one- or two-sided *Only common tests should be described solely by name; describe more complex techniques in the Methods section.*
☐	☒ A description of all covariates tested
☐	☒ A description of any assumptions or corrections, such as tests of normality and adjustment for multiple comparisons
☐	☒ A full description of the statistical parameters including central tendency (e.g. means) or other basic estimates (e.g. regression coefficient) AND variation (e.g. standard deviation) or associated estimates of uncertainty (e.g. confidence intervals)
☐	☒ For null hypothesis testing, the test statistic (e.g. *F*, *t*, *r*) with confidence intervals, effect sizes, degrees of freedom and *P* value noted *Give P values as exact values whenever suitable.*
☒	☐ For Bayesian analysis, information on the choice of priors and Markov chain Monte Carlo settings
☒	☐ For hierarchical and complex designs, identification of the appropriate level for tests and full reporting of outcomes
☐	☒ Estimates of effect sizes (e.g. Cohen's *d*, Pearson's *r*), indicating how they were calculated

Our web collection on statistics for biologists contains articles on many of the points above.

Software and code

Policy information about availability of computer code

Data collection	Oracle Clinical RDC 5.4.0
Data analysis	Software used for alignment and variant/copy number calling of whole exome sequencing data included a Sentieon Inc. implementation of GATK pipelines for alignment and copy number detection, Tnscope, Strelka2, and Control-FREEC LOH. RNA sequencing data was processed to quantify gene abundances using STAR and RSEM. Statistical analyses were conducted in R.

For manuscripts utilizing custom algorithms or software that are central to the research but not yet described in published literature, software must be made available to editors and reviewers. We strongly encourage code deposition in a community repository (e.g. GitHub). See the Nature Portfolio guidelines for submitting code & software for further information.

Data

Policy information about availability of data

All manuscripts must include a data availability statement. This statement should provide the following information, where applicable:

- Accession codes, unique identifiers, or web links for publicly available datasets
- A description of any restrictions on data availability
- For clinical datasets or third party data, please ensure that the statement adheres to our policy

WES and RNAseq datasets have been deposited in the European Genome-phenome Archive (EGA) under Study ID EGAS50000000747 and will be made available from the corresponding author upon reasonable request. Bristol Myers Squibb will honor legitimate requests for clinical trial data from qualified researchers who

submit an in-scope proposal approved by the Independent Review Committee. Before data are released, the researcher(s) must sign a Data Sharing Agreement, after which the de-identified and anonymized datasets can be accessed within a secured portal. Bristol Myers Squibb policy on data sharing may be found at https://www.bms.com/researchers-andpartners/independent-research/data-sharing-request-process.html.

Research involving human participants, their data, or biological material

Policy information about studies with human participants or human data. See also policy information about sex, gender (identity/presentation), and sexual orientation and race, ethnicity and racism.

Reporting on sex and gender	The ethics guidelines outlined are followed where applicable.
Reporting on race, ethnicity, or other socially relevant groupings	The ethics guidelines outlined are followed where applicable.
Population characteristics	Details regarding the CheckMate 649 eligibility criteria and study population characteristics have been described previously (Janjigian YY, et al. Lancet 2021;398:27-40): Eligible patients were aged 18 years or older, with previously untreated, unresectable advanced or metastatic gastric, gastroesophageal junction, or esophageal adenocarcinoma. Other key inclusion criteria were measurable (at least one lesion) or evaluable disease per Response Evaluation Criteria in Solid Tumors (RECIST), version 1.1; Eastern Cooperative Oncology Group performance status of 0 or 1; adequate organ function; and availability to provide a fresh or archival tumour sample to evaluate PD-L1. Patients with previous adjuvant or neoadjuvant chemotherapy, radiotherapy, or chemoradiotherapy (administered at least 6 months before randomisation) were eligible. Patients with known HER2-positive status; untreated CNS metastases; peripheral neuropathy (higher than grade 1); active, known, or suspected auto immune disease; positive test result for hepatitis B or C virus; and known history of positive test for HIV or known AIDS were excluded. Additional details can be found in the study protocol.
Recruitment	CheckMate 649 (NCT02872116) was conducted at 175 hospitals and cancer centers in 29 countries across Asia, Australia, Europe, North America, and South America. Overall, 3,186 patients were enrolled, and 2,031 were randomized; of these, 1,581 patients were concurrently randomized to nivolumab plus chemotherapy (789 patients) or chemotherapy (792 patients) (from April 2017 to May 2019), and 813 were concurrently randomized to nivolumab plus ipilimumab (409 patients) or chemotherapy (404 patients) (from October 2016 to June 2018). Among randomized patients, 782 received one or more dose of nivolumab plus chemotherapy, and 767 received chemotherapy; 403 patients received nivolumab plus ipilimumab, and 389 received chemotherapy. Full details were previously published. See manuscript methods and protocol for additional details.
Ethics oversight	The trial was conducted according to Good Clinical Practice guidelines developed by the International Council for Harmonisation and in compliance with the trial protocol. The trial protocol was approved by the institutional review boards or independent ethics committees at each site. All patients provided written informed consent prior to trial participation per Declaration of Helsinki principles.

Note that full information on the approval of the study protocol must also be provided in the manuscript.

Field-specific reporting

Please select the one below that is the best fit for your research. If you are not sure, read the appropriate sections before making your selection.

☒ Life sciences ☐ Behavioural & social sciences ☐ Ecological, evolutionary & environmental sciences

For a reference copy of the document with all sections, see nature.com/documents/nr-reporting-summary-flat.pdf

Life sciences study design

All studies must disclose on these points even when the disclosure is negative.

Sample size	Details regarding the statistical analyses in CheckMate 649 have been described previously (Janjigian YY, et al. Lancet 2021;398:27-40): With an assumed PD-L1 CPS ≥5 prevalence of 35%, based on limited available data, it was estimated that the primary population would consist of 554 patients. For OS, the hazard ratio (HR) was modeled as a two-piece HR, a delayed effect for the first 6 months followed by a constant HR of 0·65 thereafter, providing an average HR of 0.74. At final analysis, it was expected that 466 events would provide approximately 85% power. The HR for PFS was modeled as a two-piece HR with a delayed effect for the first 3 or 6 months followed by a constant HR of 0.56. At 12-month minimum follow-up, the expected numbers of PFS events were estimated to be 497 for a 3-month delay with approximately 99% power and 506 for a 6-month delay with approximately 60% power. Of 1,581 patients randomized to receive nivolumab-plus-chemotherapy versus chemotherapy, 685 (43%) were evaluable by whole-exome sequencing (WES), and 809 (51%) were evaluable by RNA sequencing (RNAseq). Of 813 patients randomized to receive nivolumab-plus-ipilimumab versus chemotherapy, 366 (45%) were evaluable by WES, and 402 (49%) were evaluable by RNAseq.
Data exclusions	Data analyses were conducted in the subset of patients with evaluable data for each assay type who provided informed consent. Assay results that did not pass quality control procedures (further outlined in methods) were not included.
Replication	As this is a post-hoc exploratory biomarker analysis of the CheckMate 649 study, the reproducibility of experimental findings is not applicable.

Randomization	Details regarding randomization in CheckMate 649 have been described previously (Janjigian YY, et al. Lancet 2021;398:27-40): Randomization was done using interactive web response technology (block sizes of six) and stratified according to tumor cell PD-L1 status (≥1% vs <1% or indeterminate), region (Asia vs USA and Canada vs rest of world), Eastern Cooperative Oncology Group performance status (0 vs 1), and type of chemotherapy (XELOX vs FOLFOX).
Blinding	Details regarding blinding in CheckMate 649 have been described previously (Janjigian YY, et al. Lancet 2021;398:27-40): The CheckMate 649 study was open label so investigators were not masked to treatment allocation.

Reporting for specific materials, systems and methods

We require information from authors about some types of materials, experimental systems and methods used in many studies. Here, indicate whether each material, system or method listed is relevant to your study. If you are not sure if a list item applies to your research, read the appropriate section before selecting a response.

Materials & experimental systems

n/a	Involved in the study
☐	☒ Antibodies
☒	☐ Eukaryotic cell lines
☒	☐ Palaeontology and archaeology
☒	☐ Animals and other organisms
☐	☒ Clinical data
☒	☐ Dual use research of concern
☒	☐ Plants

Methods

n/a	Involved in the study
☒	☐ ChIP-seq
☒	☐ Flow cytometry
☒	☐ MRI-based neuroimaging

Antibodies

Antibodies used	PD-L1; immunohistochemistry assay (Dako PD-L1 IHC 28-8 pharmDx assay; Agilent Technologies, Inc.)
Validation	Details can be found in the manufacturer's website: https://www.agilent.com/en-us/product/pharmdx/pd-l1-ihc-28-8-overview

Clinical data

Policy information about clinical studies

All manuscripts should comply with the ICMJE guidelines for publication of clinical research and a completed CONSORT checklist must be included with all submissions.

Clinical trial registration	NCT02872116
Study protocol	The study protocol and statistical analysis plan has been submitted as a supplemental file along with the manuscript. Proprietary information has been redacted in these documents as allowed by journal guidelines
Data collection	CheckMate 649 was conducted at 175 hospitals and cancer centers in 29 countries across Asia, Australia, Europe, North America, and South America. Study details are summarized in the Methods section. Full details were previously published.
Outcomes	Endpoints were previously published and can be found in the protocol. The biomarkers analysis performed for this manuscript were of exploratory nature.

Plants

Seed stocks	N/A
Novel plant genotypes	N/A
Authentication	N/A